

R·I·T



Rochester Institute of Technology  
Chester F. Carlson Center for Imaging Science  
Digital Imaging and Remote Sensing Laboratory

**Annual Report for the Academic Year 2010-2011**

**on the Activities of the**

**Digital Imaging and Remote Sensing Laboratory**

**Prepared by the DIRS Laboratory**

David W. Messinger, Ph.D.  
Laboratory Director

John R. Schott, Ph.D.  
Frederick & Anna B. Wiedman Professor

Digital Imaging and Remote Sensing Laboratory  
Chester F. Carlson Center for Imaging Science  
Rochester Institute of Technology  
54 Lomb Memorial Drive Rochester, NY 14623



## Contents

<b>1 Introduction</b>	<b>5</b>
<b>2 DIRS Laboratory Overview</b>	<b>7</b>
2.1 Laboratory Personnel . . . . .	7
2.1.1 Faculty . . . . .	7
2.1.2 Research & Support Staff . . . . .	8
2.1.3 Student Researchers . . . . .	9
2.2 Theses Defended in Past Year . . . . .	10
<b>3 Research Project Summaries</b>	<b>12</b>
3.1 Landsat Data Continuity Mission System Modeling with DIRSIG . . . . .	12
3.2 NASA Land Surface Temperature Product . . . . .	16
3.3 Landsat 5 & 7 Thermal Calibration . . . . .	16
3.4 MAPPs Imaging System Development . . . . .	20
3.5 Ice Characterization Using Remote Sensing Techniques . . . . .	23
3.6 Small Target Radiometry Restoration . . . . .	25
3.7 Analysis of Heavily Laden Vehicles . . . . .	26
3.8 Accurate Radiometric Temperature Measurements using Thermal Infrared Imagery of Small Targets, Physics-Based Modeling, and Companion High-Resolution Optical Image Data Sets	28
3.9 Lake Kivu Environmental Study . . . . .	30
3.10 Information Products Laboratory for Emergency Response . . . . .	32
3.11 Modeling Research for Performance-driven Multi-modal Optical Sensors . . . . .	34
3.12 Phenomenology Study of Feature Aided Tracking of Dismounts . . . . .	36
3.13 Advanced Multi-modal Scene Development . . . . .	36
3.14 Model Extraction from Oblique Airborne Imagery (NSF AIR) . . . . .	36
3.15 Enhanced Simulation of Scenarios Through the Incorporation of Process Models . . . . .	37
3.16 Dynamic Analysis of Spectral Imagery . . . . .	39
3.17 Spatial / Spectral Large Area Search Tool Development . . . . .	41
3.18 Voxelized Approaches to LIDAR Exploitation . . . . .	42
3.19 Remote Sensing for Archeological Studies of Oaxaca, Mexico . . . . .	44
3.20 Geometrically Constrained Signature Spaces for Physics-Based Material Detection . . . . .	45
3.21 Passive Infrared Detection of Aerosol Spores . . . . .	47
3.22 Modeling a Polarized LIDAR System with DIRSIG . . . . .	49

---

3.23 Improved Plume Simulation in DIRSIG . . . . .	50
3.24 3D Model Extraction and Representation . . . . .	52
3.25 DIRSIG Infrastructure . . . . .	53
3.26 Advanced Radiosity Reflectance Retrieval Support . . . . .	60
3.27 Large Area Polarimetric Scene Simulation and Phenomenology . . . . .	60
3.28 SOFIA Data Cycle System Development & Support . . . . .	61
3.29 Rx-Cadre Experiments . . . . .	64
3.30 Development of 3-dimensional Air Flow Sensors for Combustion Research . . . . .	64
3.31 Enhanced Infrared and LIDAR Capabilities for Wildland Fire Research . . . . .	65
3.32 Precision Wildland Fuel Fire Experiments . . . . .	65
3.33 Improved Diagnostics for Fire-Initiation Experiments . . . . .	67
<b>4 Publications During This Period</b>	<b>70</b>

## List of Figures

2.1-1	DIRS SPIE Booth	8
2.1-2	DIRS Luau	9
2.1-3	Kelly Canham wins DigitalGlobe Award	10
2.1-4	A rooftop experiment	11
2.2-5	DIRS students	12
3.1-6	Layout of simulated Lake Tahoe scene	13
3.1-7	DIRSIG simulated Lake Tahoe scene	13
3.1-8	LDCM TIRS jitter spectra modeling	14
3.1-9	Lake Tahoe scene simulated with TIRS jitter	15
3.1-10	TIRS surface temperature regression technique	15
3.2-11	Atmospheric apparent temperature error	17
3.2-12	Spatial interpolation of NARR points	17
3.3-13	2010 Landsat ETM+ collected data	18
3.3-14	Aggregate 1999 - 2009 Landsat ETM+ validation results	19
3.3-15	2010 Landsat 5 TM calibration results	19
3.3-16	2009 - 2010 Landsat 5 calibration results	20
3.3-17	Landsat 5 calibration results by date	20
3.4-18	Multispectral polarimetric imaging system	21
3.4-19	Imagery from MAPPS sensor	22
3.5-20	ALGE surface temperature predictions for the Midland Cogeneration Venture cooling pond	24
3.5-21	Calibrated temperature maps from WASP sensor	24
3.6-22	MuSES simulations of a metal container on a concrete slab	26
3.7-23	Flatbed truck used in heavy vehicle experiment	27
3.7-24	Tractor trailer used in heavy vehicle experiment	28
3.7-25	IR image of front disc brake	28
3.7-26	IR image of rear drum brake	29
3.8-27	Geometry manipulation interface in Blender	29
3.9-28	Mosaic of 2 Landsat scenes covering Lake Kivu, Rwanda	31
3.10-29	Map product of Dai-ichi nuclear power plant	33
3.10-30	Imagery collected after Hurricane Irene	34
3.10-31	Imagery collected after Tropical Storm Lee	35
3.15-32	Road and parking lot detection and identification	38

3.15-33	DIRSIG Process Model workflow	39
3.16-34	Euclidean Commute Time Distance transformation example	40
3.17-35	Scale space tree representations of spectral imagery	42
3.18-36	Voxel models of the RIT campus from LIDAR imagery	43
3.18-37	Voxelized LIDAR line of sight map of RIT campus	44
3.19-38	Example spectral unmixing of Worldview-2 imagery	46
3.20-39	Shape factor maps derived from LIDAR	47
3.20-40	HSI/LIDAR detection software	48
3.21-41	Aerosol cloud modeling scene layout	48
3.21-42	Aerosol radiance curves	49
3.22-43	DIRSIG LIDAR scene considerations	50
3.23-44	Blackadar plume model example	51
3.23-45	Visualization of plume temperatures	51
3.23-46	DIRSIG plume model integration flowchart	52
3.23-47	Simulated on and off plume pixels	53
3.24-48	Structure from motion workflow	54
3.24-49	WASP collect footprints over RIT	55
3.24-50	Automatically extracted point cloud of RIT campus	56
3.25-51	DIRSIG “warehouse” scene in Blender	57
3.25-52	DIRSIG “warehouse” scene rendering	57
3.25-53	DIRSIG “refinery” scene in Blender	58
3.25-54	DIRSIG “refinery” scene rendering	59
3.26-55	Modeled and experimental radiosity scene	60
3.27-56	Large scale DIRSIG polarimetric scene	61
3.28-57	Mid-infrared image of the Orion nebula (M42)	62
3.28-58	Terahertz spectroscopy of the M17 star forming region	63
3.32-59	Wildfire angular distribution experiment	66
3.32-60	Wildfire emissivity experimental setup	67
3.32-61	Wildfire radiant fraction experiment setup	67
3.33-62	Wildfire initiation experiment setup	69

## 1 Introduction

Once again, another year has passed at RIT, and for the Digital Imaging and Remote Sensing Laboratory it was a very busy, and significant year. We successfully integrated the two “remote sensing” laboratories, the Laboratory for Imaging Algorithms and Systems (LIAS) and DIRS, into one entity under the name DIRS. This effort was started in the spring of 2010 and finalized in the 2010-2011 academic year. DIRS now numbers nine full time faculty in CIS (plus several more collaborators across RIT), over 15 full time administrative, support, and technical staff, and over 40 students at the undergraduate and graduate levels. The research program continues to be both broad and deep, spanning over 40 research projects and several imaging modalities and application areas. It is the depth and breadth of the research program that maintains DIRS as one of the premier research laboratories devoted to remote sensing in the world.

A major accomplishment as we integrated the two groups was space consolidation. The LIAS group occupied space in a separate building, not in the Center for Imaging Science facilities. Over the course of the fall of 2010, a “space swap” was arranged between several research groups, resulting in DIRS acquiring some excellent (and newly renovated!) lab space, as well as permanent offices for all DIRS personnel in the Center for Imaging Science building. This has resulted in an outstanding level of collaboration both within the group, and between the DIRS personnel and the rest of the Center. The advantages of this setup can not be overstated, and we owe a great deal of thanks to the RIT administration for facilitating the space swap and renovation.

Amongst the faculty and staff members of the lab there were several milestones. Scott Brown, a long time member of the research staff in DIRS and the lead scientist on all things DIRSIG, completed his Ph.D. in Environmental Engineering from the University of Buffalo in the spring of 2011. Congratulations to Scott on a major accomplishment! Dr. John Kerekes was elected to the IEEE Geoscience and Remote Sensing Administrative Committee was appointed as the Vice President of Technical Activities for the Society. Additionally, several members of the group served on various review panels for both government and industry and continue to serve as peer reviewed journal associate editors and reviewers. Also, I was asked to serve as the Academic Advisor to the Remote Sensing Advisory Board for the US Department of Homeland Security.

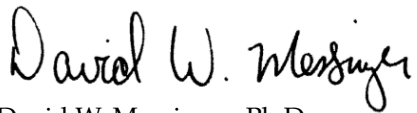
DIRS continues to increase its scholarly output as well. In the past year, members of the DIRS laboratory have attended over 15 different (international) conferences and presented over 35 presentations. The group has published over 60 refereed journal and conference proceedings papers, one book chapter, and Dr. Emmett Ientilucci and Dr. John Schott have a book under contract with SPIE. A full list of DIRS publications for 2010 - 2011 is provided at the end of this report.

The DIRSIG team have started to take DIRSIG Training “on the road,” having offered four training classes to over 50 attendees last year. Two of the training sessions were held at RIT, while one was held in Herndon, VA and the other was held in the San Francisco, CA area. They have also been busy engaging their user community through the DIRSIG blog, and they now have approximately 200 - 250 users of the simulation.

In other research news, the DIRS lab joined the National Ecological Observatory Network (NEON) Consortium. This NSF funded project engages over 50 universities, providing policy, experimental design, product support, and science support. RIT will focus on waveform LIDAR processing and products, calibration of the NEON sensors, and potentially providing airborne thermal imaging capabilities. We also furthered our work in disaster response by providing support to the US Geological Survey’s efforts to support the response to the March 2011 Japanese Earthquake and Tsunami disaster. DIRS provided image analysis and map support to the effort, producing several high resolution image-derived maps that were delivered to first responders in Japan.

I also want to highlight international awards won by three Imaging Science graduate students performing their research in the DIRS laboratory, all Ph.D. candidates. Kelly Canham and Nima Pehlaven both won the Alexander Goetz award from the Advanced Spectral Devices company. The winners of this competition were given access to ASD equipment to further their research. Nima used his award to study the use of NASA satellites to assess water quality and Kelly will be taking her spectrometer award to Oaxaca, Mexico to further her research in support of an archeology project. Kelly also won the DigitalGlobe "8 Band Challenge", seeking novel algorithmic approaches to using the new Worldview-2 satellite launched by DigitalGlobe in the fall of 2010. Kelly won for her algorithm utilizing a local spectral unmixing approach to multispectral imagery. And finally, Lingfei Ming won the IEEE data fusion award for his use of multilook imagery. His award was presented at the 2011 International Geoscience and Remote Sensing Symposium (IGRSS) in Vancouver, Canada.

I want to thank all members of the DIRS laboratory for their continued hard work and excellence. It is only through the advances made by the faculty, staff, and most importantly, the students, that we continue to be a leader in the remote sensing community.



David W. Messinger, Ph.D.  
Associate Research Professor  
Director, Digital Imaging and Remote Sensing Laboratory  
Chester F. Carlson Center for Imaging Science  
Rochester Institute of Technology

## 2 DIRS Laboratory Overview

The Digital Imaging and Remote Sensing (DIRS) Laboratory is a research group within the Chester F. Carlson Center for Imaging Science. Our work focuses on the development of hardware and software tools to facilitate the extraction of information from remotely sensed data of the earth and the education of students who will continue this work for academia, government agencies, and private industry.

The DIRS group is made up of faculty and research staff working with over 40 students ranging from High School interns, to RIT students from the Baccalaureate through Doctoral level. Most students are degree candidates in Imaging Science, but students from other departments, such as Engineering and Mathematics, are often part of the student population supporting our research initiatives.

### 2.1 Laboratory Personnel

#### 2.1.1 Faculty

*Dr. Emmett Ientilucci*, Assistant Research Professor,

Research Interests: Multi- and hyperspectral algorithm development; physics-based signature detection in hyperspectral imagery; low-light level imaging systems

Contact Information: [ientilucci@cis.rit.edu](mailto:ientilucci@cis.rit.edu); 585-475-7778

*Dr. John Kerekes*, Associate Professor

Research Interests: Image processing and algorithm development; image chain modeling and parametric analysis

Contact Information: [kerekes@cis.rit.edu](mailto:kerekes@cis.rit.edu); 585-475-6996

*Dr. Bob Kremens*, Associate Research Professor,

Research Interests: Remote sensing characterization of forest fires; in-situ measurement systems; fusion of in-situ and remote measurements

Contact Information: [kremens@cis.rit.edu](mailto:kremens@cis.rit.edu); 585-475-7286

*Dr. David Messinger*, Associate Research Professor, DIRS Laboratory Director

Research Interests: Multi- and hyperspectral algorithm development; advanced mathematical approaches to spectral image processing

Contact Information: [messinger@cis.rit.edu](mailto:messinger@cis.rit.edu); 585-475-4538

*Dr. Harvey Rhody*, Professor,

Research Interests: Image processing algorithms and systems; three-dimensional imaging

Contact Information: [rhody@cis.rit.edu](mailto:rhody@cis.rit.edu); 585-475-6215

*Dr. Carl Salvaggio*, Associate Professor

Research Interests: Novel techniques and devices for optical property measurement; applied image processing and algorithm development; image simulation and modeling

Contact Information: [salvaggio@cis.rit.edu](mailto:salvaggio@cis.rit.edu); 585-475-6380

*Dr. John Schott*, Frederick and Anna B. Wiedman Professor

Research Interests: Hyperspectral data analysis and algorithm development; multi and hyperspectral instrument development; synthetic scene simulation and modeling

Contact Information: [schott@cis.rit.edu](mailto:schott@cis.rit.edu); 585-475-5170

*Dr. Jan van Aardt*, Associate Professor,

Research Interests: Application of imaging spectroscopy and LIDAR for spectral-structural characterization of natural systems



**Contact Information:** vanaardt@cis.rit.edu; 585-475-4229

**Dr. Tony Vodacek**, Associate Professor

**Research Interests:** Environmental applications of remote sensing; forest fire detection and monitoring; active and passive sensing of water quality

**Contact Information:** vodacek@cis.rit.edu; 585-475-7816



**Figure 2.1-1: Members of the DIRS team work the booth at the 2011 SPIE Defense & Security Symposium in Orlando, FL.**

### 2.1.2 Research & Support Staff

Dr. Scott Brown: brown@cis.rit.edu; 585-298-9505

Mr. Steve Cavilia: cavilia@cis.rit.edu; 585-475-4215

Mr. Chris DeAngelis: deangelis@cis.rit.edu; 585-475-4215

Mr. Jason Faulring: faulring@cis.rit.edu; 585-475-4432

Dr. Michael Gartley: gartley@cis.rit.edu; 585-475-7194

Dr. Aaron Gerace: gerace@cis.rit.edu; 585-475-4388

Dr. Adam Goodenough: goodenough@cis.rit.edu

Mr. Bob Krzaczek: krz@cis.rit.edu; 585-475-7196

Mr. Don McKeown: mckeown@cis.rit.edu; 585-475-7192

Ms. Erin Ontiveros: ontiveros@cis.rit.edu; 585-475-4465

Ms. Nina Raqueño: nina@cis.rit.edu; 585-475-7676

Dr. Rolando Raqueño: rolando@cis.rit.edu; 585-475-6907

Mr. Michael Richardson: richardson@cis.rit.edu; 585-475-5294

Ms. Cindy Schultz: schultz@cis.rit.edu; 585-475-5508

Mr. Andy Scott: arspci@cis.rit.edu; 585-475-5508  
 Ms. Melanie Warren: mawpci@cis.rit.edu; 585-475-5508  
 Ms. Amanda Zeluff: amzpci@cis.rit.edu; 585-475-5170

### 2.1.3 Student Researchers



**Figure 2.1-2: DIRS faculty, staff, and students celebrate the successful SHARE experimental campaign with a “traditional” Rochester Luau in front of the Center for Imaging Science.**

Students pursuing research in the DIRS laboratory as of June 30, 2011:

#### **BS (12)**

Edward Amsden	Luca Ashok	Colin Axel
Tim Garvin	AnneMarie Giannandrea	Michal Kucer
Jonathan Lueders	Jessica Maben	Michael Rodgers
Kyle Ryan	Phil Salvaggio	Linnea Tullson

#### **MS (8)**

Javier Concha	Bo Ding	Michael Harris	James Letendre
Josh Zollweg	Jie Zhang	Ming Zhang	Tingfang Zhang



Figure 2.1-3: Kelly Canham, Imaging Science Ph.D. student, wins the DigitalGlobe international “8 Band Challenge” competition. The award was announced at the ESRI User Group Meeting in San Diego.

#### Ph.D. (26)

Jamie Albano	Bikash Basnet	Madhurima Bandyopadhyay	Kelly Canham
Bin Chen	Jake Clements	Monica Cook	Shea Hagstrom
Jared Herweg (USAF)	David Kelbe	Sanjit Maitra	Troy McKay
Lingfei Meng	Ryan Mercovich	David Nilosek	Nima Pahlevan
Sarah Paul	Paul Romanczyk	Shagan Sah	Katie Salvaggio
Jiangqin Sun	Shaohui Sun	Weihua Sun	William Wu
Jiashu Zhang	Amanda Ziemann		

## 2.2 Theses Defended in Past Year

- Annette Rivas, MS, “Tunable micro-electro mechanical fabry perot etalon”
- Cliff Anderson, Ph.D., “ Renement of the Method for Using Pseudo-Invariant Sites for Long Term Calibration Trend- ing of Landsat Reective Bands”



**Figure 2.1-4: Sanjit Maitra, a DIRS student, performs an experiment on the roof of the Center for Imaging Science.**

- X. Fan, Ph.D., “Automatic Registration of Multi-Modal Airborne Imagery”
- Brian Flusche, Ph.D., “An Analysis of Multimodal Sensor Fusion for Target Detection in an Urban Environment”
- Michael Presnar, Ph.D., “Modeling and Simulation of Adaptive and Multimodal Optical Sensors for Target Tracking in the Visible to Near Infrared”
- Jacqueline Speir, Ph.D., Validation of 3D Radiative Transfer in Coastal Ocean-Water Systems as Modeled by DIRSIG”
- Alvin Spivey, Ph.D., “Land Cover Land Use Change Index Interpretation for the Persistent Monitoring of Riparian System Landscape Pattern When Using Multiple Sensor Scales”
- Aaron Weiner, Ph.D., “A Systems Level Characterization and Tradespace Evaluation of a Simulated Airborne Fourier Transform Infrared Spectrometer for Gas Detection”
- Chabitha Devaraj, Ph.D., “Polarimetric Remote Sensing System Analysis: DIRSIG Model Validation and Impact of Polarization Phenomenology on Material Discriminability”
- Karl Walli, Ph.D., “Relating Multimodal Imagery Data in 3D”



Figure 2.2-5: DIRS students in summer of 2011.

### 3 Research Project Summaries

#### 3.1 Landsat Data Continuity Mission System Modeling with DIRSIG

Sponsor: NASA - Goddard Space Flight Center

Principal Investigator(s): Dr. John Schott

Research Team: Dr. Aaron Gerace, Dr. Michael Gartley, Dr. Scott Brown

Project Description:

This project provides support to the Landsat Data Continuity Mission (LDCM) with an emphasis on modeling radiometric and image quality issues associated with two new sensors to be flown on the next Landsat satellite. While year one of this work focused on developing the DIRSIG capabilities necessary to model the geometric properties of the Operational Land Imager (OLI) and the Thermal Infrared Sensor (TIRS), year two efforts have focused on using the model to identify image quality issues associated with the sensors.

Project Status:

Several studies were conducted in year 2 of this effort to gauge the potential image quality of LDCM and to identify/model issues that may impact this image quality. These studies included:

***Addressing the potential for banding on TIRS.***

Figure 1 shows the simulated landscape that was used in this study to help identify potential banding issues associated with the TIRS instrument. NASA measured the relative spectral response functions for each detector on the TIRS flight instrument and provided 4 (2 per band) that represented extreme cases. RIT used these 4 RSRs as input to DIRSIG and imaged over the simulated landscape shown in Figure 3.1-6 (which included calibration panels of varying temperatures and emissivities) for a range of atmospheres. The resulting data was analyzed by both RIT and NASA and it was determined that banding would not

likely be an issue with the TIRS data.

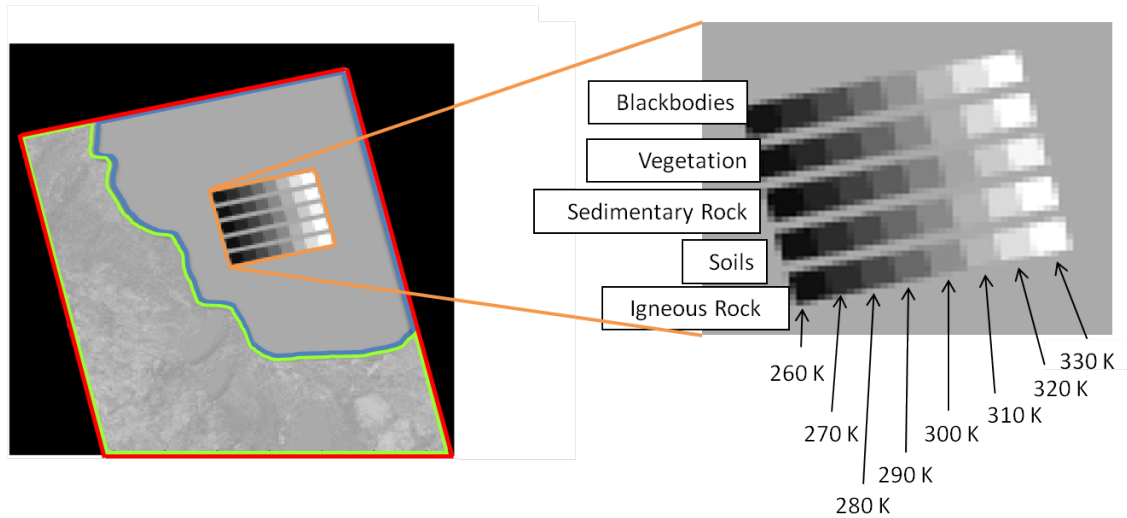


**Figure 3.1-6: The simulated Lake Tahoe landscape (designed with calibration panels of varying temperatures and emissivities) that was used to determine the potential for banding of TIRS image data.**

#### *Registration of synthetic OLI data.*

OLI registration algorithms were provided by NASA and used by RIT to produce terrain corrected, georectified synthetic images for each OLI spectral band. Figure 3.1-7 shows an RGB image of a DIRSIG rendering of the Lake Tahoe landscape where the spectral bands have been registered using the NASA-provided algorithms.



**Figure 3.1-7: DIRSIG rendering of the Lake Tahoe landscape that has been registered using RIT's implementation of NASA-provided registration algorithms.**

*Evaluating the impact of jitter (originating from the TIRS cryo-cooler) on LDCM data.*

A major portion of this year 2 effort focused on determining if jitter due to the TIRS cryo-cooler would impact the TIRS and OLI image data. A jitter capability was implemented into the DIRSIG model and validated using DIRSIG's ephemeris data output. Figure 3.1-8 illustrates the model validation where the cross-track jitter spectra that was measured and provided by NASA (black) was used as input to the model and DIRSIG's data recorder tool used to retrieve the observed spectra (dashed green).

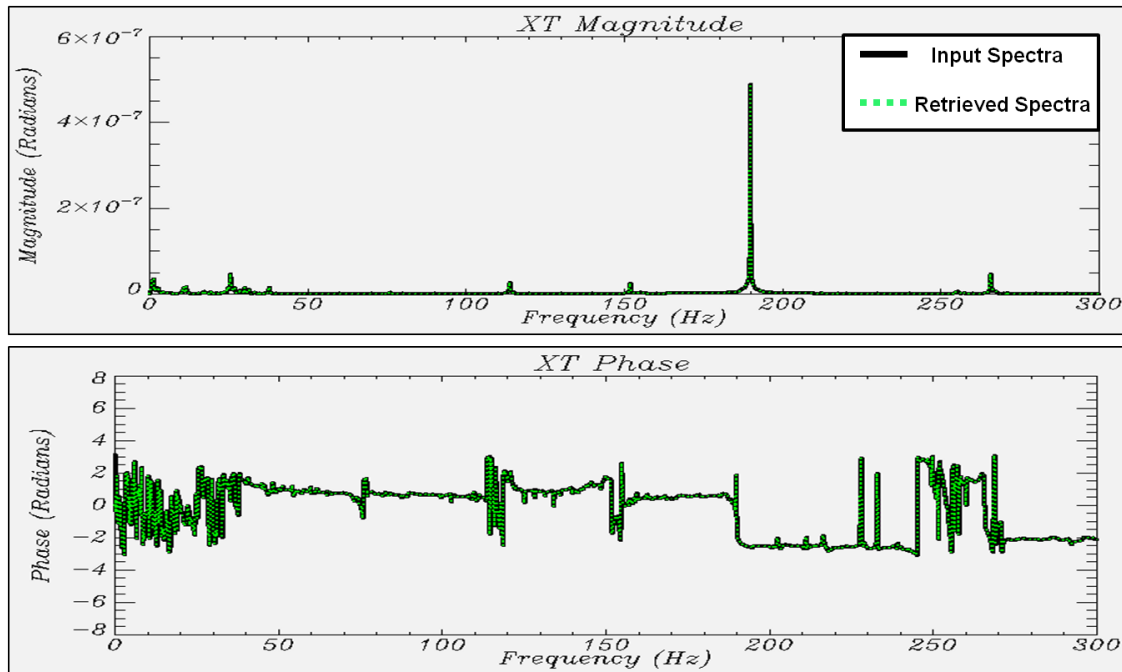


**Figure 3.1-8: (Black) NASA measured and provided jitter spectra that was used as input to the model. (Dashed green) Corresponding jitter spectra that was recovered from the model.**

With a validated model in place, a modified version of the Lake Tahoe synthetic landscape (Figure 4) was developed in order to measure the geometric impact of jitter on LDCM image data. It was determined that, given the existing spectra, jitter originating from the TIRS cryo-cooler should not have a significant impact on LDCM image quality.

*Development of a split-window technique for the TIRS instrument to determine surface temperature.*

This work represents an ongoing effort to develop a split window technique, in support of the TIRS instrument, that effectively compensates for the atmosphere in an effort to retrieve land surface temperatures. Regressions are developed for a variety of atmospheric/material emissivity conditions (in the absence of radiosonde data) and serve as a tool to invert apparent temperature in the 2 bands of TIRS to surface temperature. One such regression (shown in Figure 5) illustrates that, on average, land surface temperature can be determined to within 0.89K in the absence of radiosonde data. By manipulating the regression data, temperature retrieval errors may be as low as 0.75K under certain conditions.

Ongoing efforts for this project focus on calibrating the LDCM data to support the post-launch data products. Detector-to-detector non-uniformities are being modeled in DIRSIG and an emphasis placed on correcting the raw image data. The side-slither technique is being investigated in DIRSIG in an effort to correct for potential detector-to-detector non-linearities.

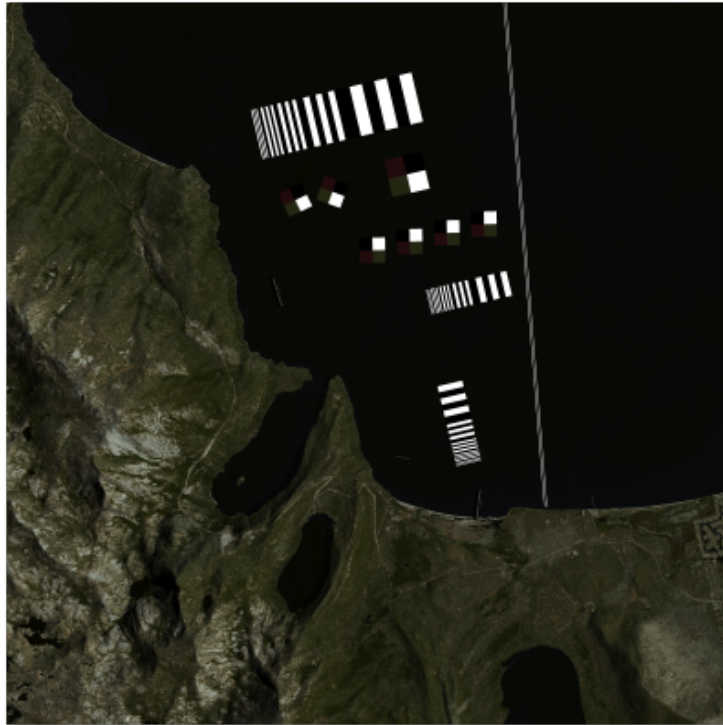


Figure 3.1-9: Modified synthetic Lake Tahoe landscape that was used to measure the impact of TIRS jitter on LDCM image data.

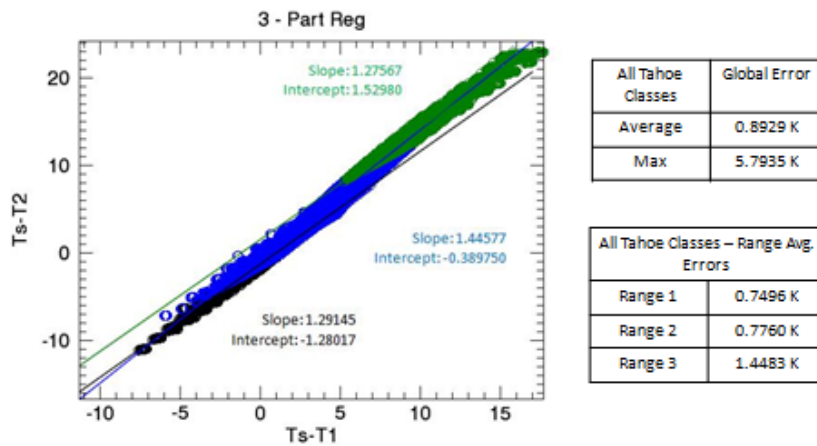


Figure 3.1-10: Regression developed for a variety of atmospheric/material emissivity conditions that can be used to retrieve land surface temperature to within 0.75K, on average.



### 3.2 NASA Land Surface Temperature Product

Sponsor: NASA, JPL, NASA Goddard, USGS EROS

Principal Investigator(s): Dr. John Schott

Research Team: Monica Cook (CIS - Ph.D.)

Project Description:

Land Surface Temperature (LST) is an important Earth System Data Record for many applications and areas of research, including environmental models, numerical weather prediction, and climatic variability. The goal of this work is to develop a LST product for the Landsat archives from Landsat-4 to the currently collecting Landsat-5 and Landsat-7. The spatial and temporal resolution of the Landsat series, as well as the historical and projected future coverage, makes it an optimal satellite series for a product of this nature. The single thermal band of the Landsat satellites is largely under-utilized because both the emissivity and a characterization of the atmospheric profile are necessary in order to extract the temperature. A newly available high resolution, seasonal emissivity database derived from ASTER data will be combined with atmospheric characterizations produced using radiative transfer code to compute the LST for this product.

With the necessary atmospheric characterization (pressure, temperature, and water vapor content), a radiative transfer code (MODTRAN) can be used to generate the atmospheric parameters (upwelled radiance, downwelled radiance, and transmission) required to compute the LST. This is the main focus of this research. The North American Regional Reanalysis (NARR) program provides this atmospheric profile data covering the spatial and temporal range of the Landsat series. To calculate the LST for each pixel, this data needs to be input into the radiative transfer code and interpolated both spatially and temporally to match the resolution of the Landsat scenes.

The bulk of current work focuses on assessing interpolation techniques by calculating the error in apparent temperature. The NARR data must be adjusted to the appropriate elevation for the Landsat pixel under consideration. Initial work shows that truncating layers below the pixel elevation and linearly interpolating to the ground altitude provides acceptable results. As shown in Figure 3.2-11, this technique can introduce as little as 0.2 K error in apparent temperature. The data must also be interpolated in time to the acquisition of the Landsat scene; the NARR data is available in 3-hour increments and can be linearly interpolated to the time of the Landsat acquisition. Finally, the atmospheric parameters must be interpolated in space to the UTM coordinates of each pixel. As shown in Figure 3.2-12, NARR data is available at 32 km centers and initially an inverse distance weighting interpolation of the four nearest points will be explored.

Project Status:

This project is in the first year of a three year effort. This is a joint project with NASA JPL who will focus on the emissivity component with RIT focused on the atmospheric compensation. The first year is targeted at generation of an approach appropriate for North America. Initial interpolation approaches have been implemented but require further assessment. Error will be calculated by comparison to available ground truth data. Future work also includes implementing processes to appropriately filter the atmospheric data.

### 3.3 Landsat 5 & 7 Thermal Calibration

Sponsor: NASA, USGS

Principal Investigator(s): Dr. John Schott

Research Team: Nina Raqueño

1 February 2007

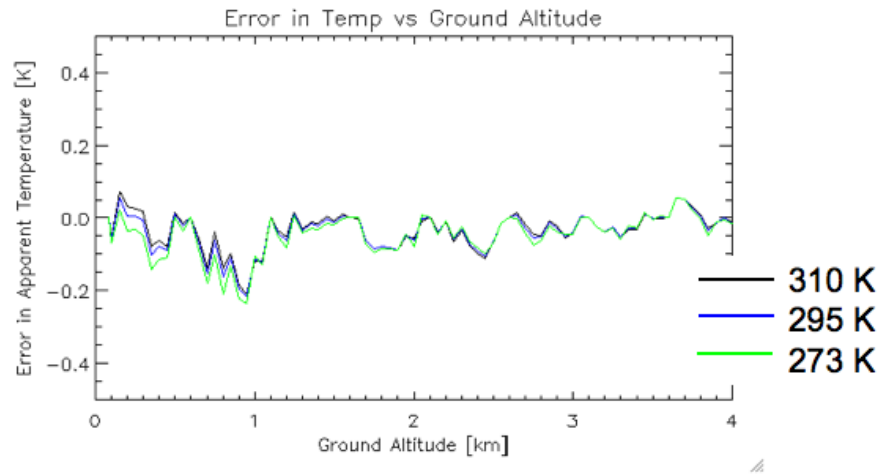


Figure 3.2-11: Plot of error in apparent temperature vs. ground altitude as the atmospheric layers were truncated and the bottom layer was interpolated to the appropriate ground altitude.

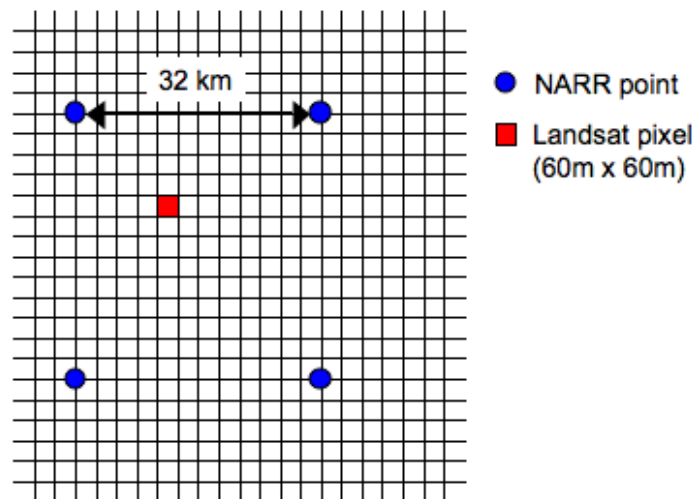


Figure 3.2-12: Illustration of spatial interpolation between 4 nearest NARR points to each Landsat pixel.

Project Description:

RIT continued to monitor the current calibration of Landsat 5 & 7 Thermal bands with surface temperatures taken on Lake Ontario and Lake Erie, as well as, supplemental NOAA buoy temperatures.

***Landsat 7 Thermal Calibration Results***

Ground truth surface water temperatures ranging between 6.6 to 20.4 degrees Celsius were collected on

Lake Ontario and Lake Erie between the months of April and July. The analysis of the 2010 data was further supplemented with buoy corrected temperatures that were converted to surface-leaving radiances and extrapolated to space using MODTRAN. The results are presented by plotting the image derived radiance and the ground truth radiance for 19 individual samples (Figure 3.3-13). The 2010 data indicate an average bias error of 0.017 [w/m<sup>2</sup> sr mm] which is equivalent to a temperature bias of 0.14 K. This data indicates that the Landsat ETM+ thermal band 6 is still operating nominally over typical temperatures encountered on the earth's surface.

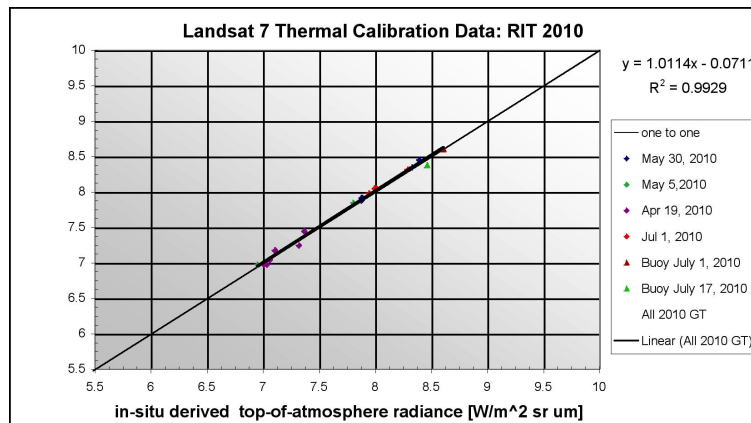


**Figure 3.3-13: Plot of predicted versus observed at sensor radiance for Landsat ETM+ data collected during the 2010 season.**

The results from an independent team indicated that at high temperatures (40C) the difference between satellite and vicarious temperatures was significant indicating a potential gain. Although RIT does not expect to observe samples at such high temperatures at its calibration sites, the RIT data also indicates a gain may be present at such high temperatures. Figure 3.3-14 presents RIT's thermal calibration results from launch through 2009. RIT's complete dataset also indicates a slight gain with a regression fit of  $y = 0.9498x + 0.364$  which is comparable to the independent dataset which resulted in a regression fit of  $y = 0.957x + 0.324$ . The combined data indicate that for most users ETM+ band 6 is calibrated but for users interested in hot environments the satellite may be underestimating temperatures.

Given that the results from the two independent teams are in agreement and have been consistent over many years of monitoring it was recommended that the datasets be pooled to determine a recommended gain correction. On January 1st, 2010, the calibration of the ETM+ thermal band was modified to correct for this lifetime gain error through a change in the Calibration Parameter File.

#### **Landsat 5 Thermal Calibration Results**

During 2010, surface water temperatures ranging between 1.3 to 15.7 degrees Celsius were collected on Lake Ontario and Lake Erie between the months of April and October. The results are presented by plotting the image derived radiance and the ground truth radiance for 16 individual samples (Figure 3.3-15). A regression line is then fitted to the data and compared to the ideal calibration one to one line. The 2010 data indicate an overall bias error of -0.015 [w/m<sup>2</sup> sr mm] which is equivalent to a temperature bias of 0.13 K. Figure 3.3-16 presents the calibration results in terms of Bias Temperature. This data indicates that the Landsat 5 thermal band 6 is still operating nominally and within the measurement error of this process. This agreement between satellite predicted and truth is expected since this analysis includes the recommended bias and gain correction that was implemented starting April 1st, 2010.

During the spring months of 2011, RIT continued to monitor Landsat 5 thermal calibration by collecting

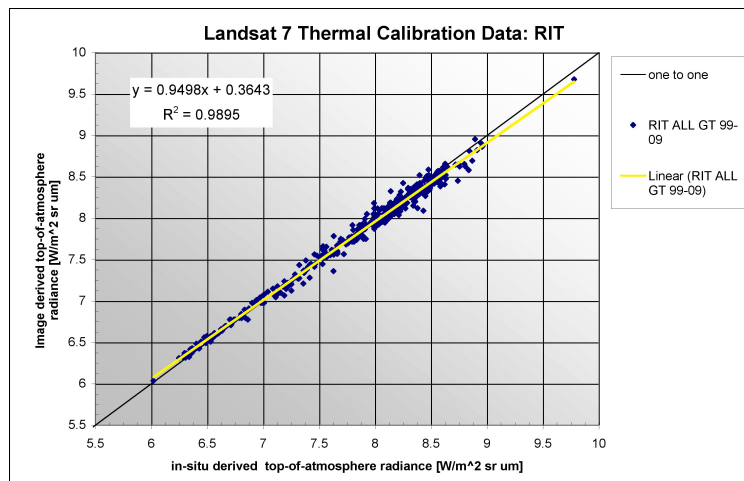


Figure 3.3-14: The 1999-2009 combined results from ten years of validation of Landsat ETM+.

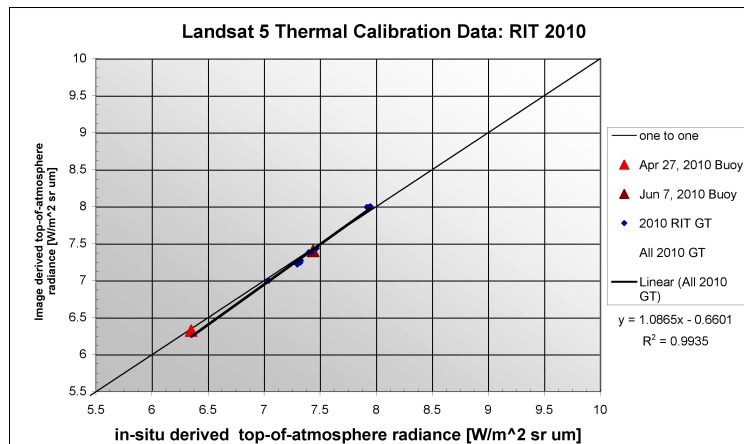


Figure 3.3-15: 2010 Landsat 5 TM thermal calibration results of satellite predicted radiances compared to truth.

additional ground truth on Lake Ontario. This was supplemented with coastal buoy data during the winter months. Figure 3.3-17 highlights newly processed buoy data from November 2009-March 2011.

#### Project Status:

RIT continues to monitor the thermal accuracy of both of the active Landsat instruments (5 & 7). The results generated from Great Lakes ground truth and the NOAA buoy methodology are presented to NASA's Landsat Calibration Team twice annually.

With the anticipation of the launch of Landsat Next, RIT is converting the manual buoy calibration process into an automated workflow.

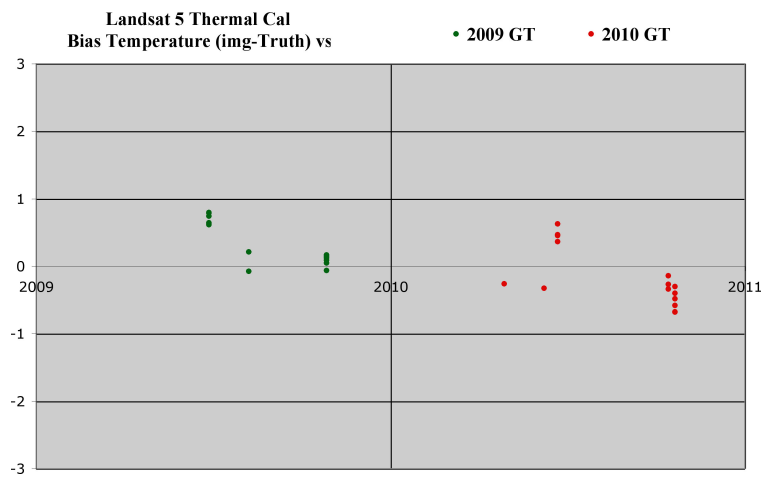


Figure 3.3-16: 2009-2010 Landsat 5 thermal calibration results presented in terms of bias temperatures.

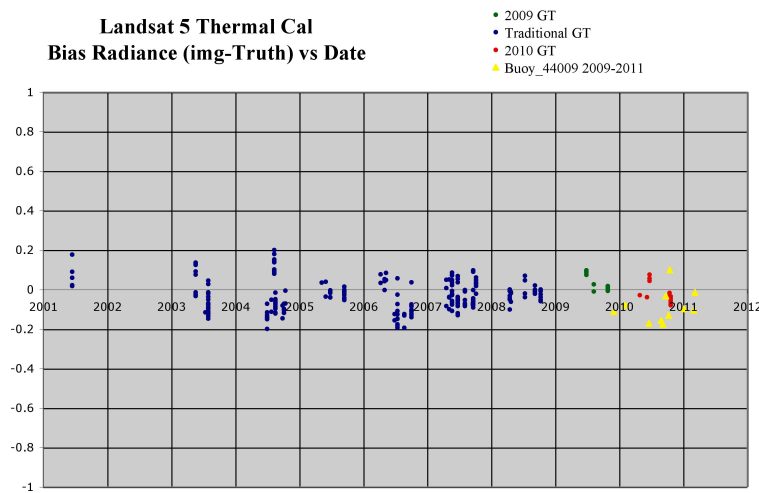


Figure 3.3-17: Landsat 5 thermal calibration results presented as Bias Temperatures by Date. This plot highlights (yellow) the benefits of including buoy data from year round coastal sites.

### 3.4 MAPPS Imaging System Development

Sponsor: Intelligence Community Postdoctoral Fellowship

Principal Investigator(s): Dr. Carl Salvaggio

Research Team: Dr. Brent Bartlett, Jason Faulring

Project Description:

A new sensor was proposed to provide a unique collection capability, allowing for high-resolution spectro-polarimetric aerial imagery to be collected. The requirements for this system, termed the Multispectral Aerial Passive Polarimeter (MAPPS), were defined to allow the collection of the linear polarization state of

observed radiation for up to ten spectral bands. The system operates in either the laboratory, the field, or from an airborne platform to allow for many different types of scene scenarios to be explored.

The operational system can collect imagery of outdoor scenes to identify key observables in spectro-polarimetric data for various tasks. Anomaly detection was performed using the preliminary spectro-polarimetric data to identify man-made objects. An emphasis will be placed on determining algorithmic sensitivity for ground sample distance, spectral response, and target contaminant levels.

#### Project Status:

MAPPS is a division of time polarimeter consisting of a high resolution JAI BM-500GE CCD camera with a Schneider Optics lens coupled to a Sutter Lambda 10-3 dual filter wheel with ten slots per wheel. The digital camera acquires 12-bit imagery with a resolution of 2456x2058 pixels with a 3.45 $\mu$ m pixel pitch using a 35mm focal length giving high spatial resolution. The first filter wheel contains a set of linear polarizers, each oriented with their transmission axes rotated relative to each other. The second filter wheel contains a set of spectral bandpass filters allowing for up to 10 different spectral bands to be collected. For each spectral filter the linear polarizer set is rotated, thus allowing for spectral Stokes imagery to be generated. Figure 3.4 shows a top view of the system as well as the system mounted to a tripod.

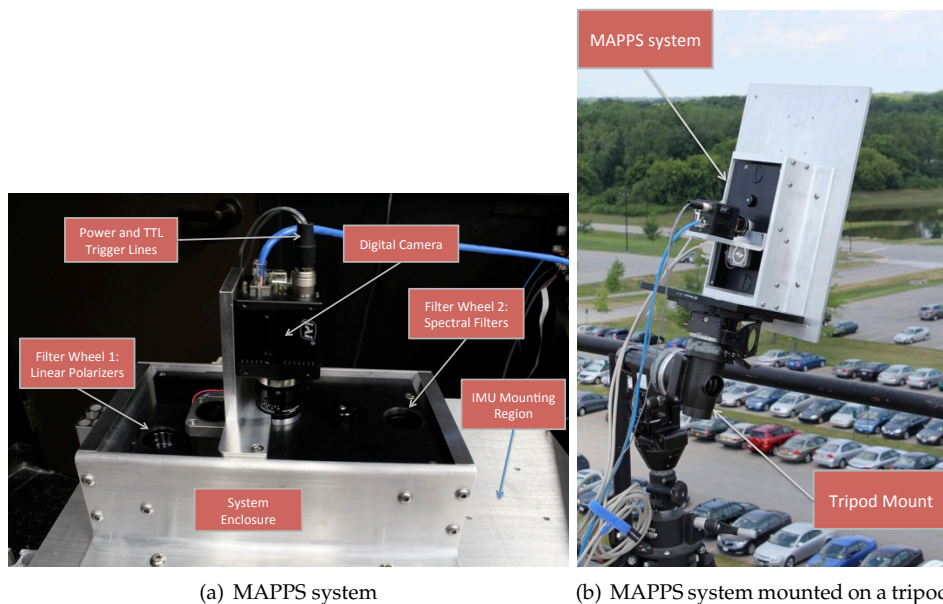


**Figure 3.4-18: MAPPS system consisting of a dual filter wheel and gigabit ethernet camera.**

Preliminary imagery was collected from the rooftop of a building to test the system in a complex outdoor environment. A parking lot was imaged containing a mixture of asphalt and grass backgrounds along with a parked vehicle and a panel cluster[19]. The panel cluster has various painted regions comprising different surface finishes and colors. The panel surfaces can also be set a different angles to face different portions of the skydome. Figure 3.4 shows a cropped portion of the imagery that was captured in a backscattering geometry relative to the sun principle plane. The S1 and S2 imagery shows how the different panels have different Stokes values depending on which portion of the hemisphere is sampled with the given source / detector geometry. This is expected since the skydome has significant polarization. The results of running TAD-PCA are also shown which indicate that various anomalous materials can be identified relative to the background parking lot and grass with this system.

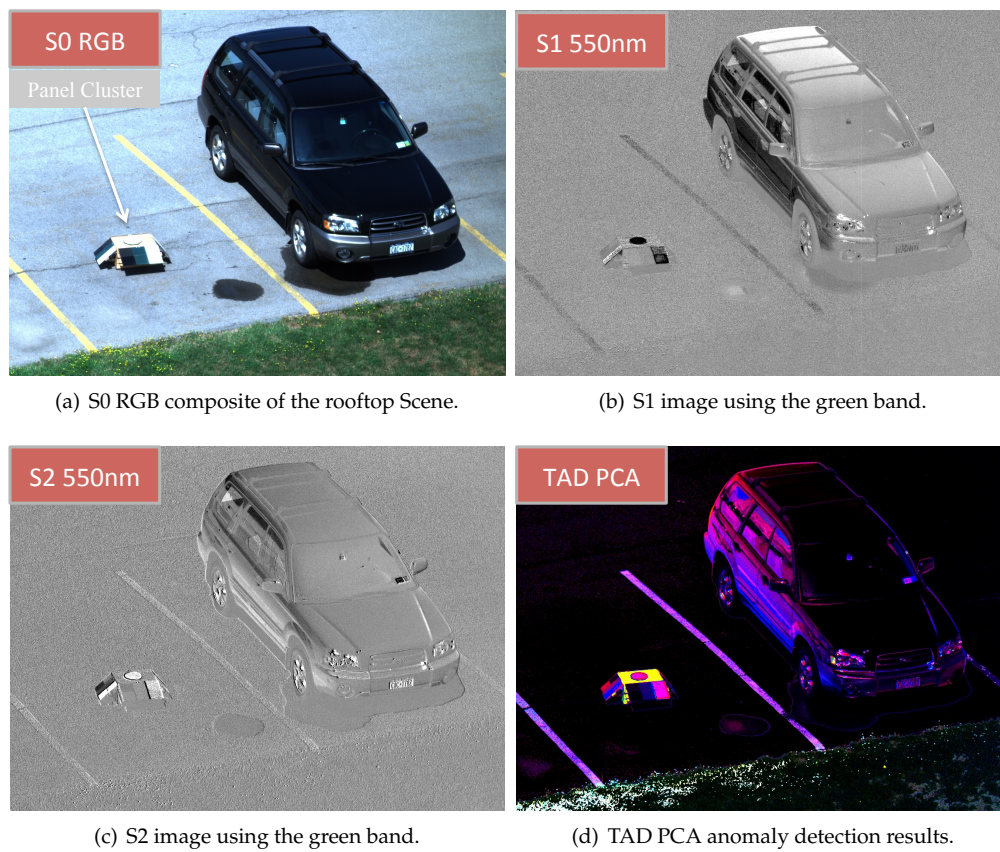


**Figure 3.4-19: Rooftop scene imaged with MAPPS sensor.**

### 3.5 Ice Characterization Using Remote Sensing Techniques

Sponsor: DOE

Principal Investigator(s): Dr. Carl Salvaggio

Research Team: May Casterline (CIS - Ph.D.), Jason Faulring, Mike Richardson

Project Description:

Water environments exposed to below freezing conditions present a challenge to standard thermal calibration techniques. Any water present can exist in several different states simultaneously within a scene: liquid water, solid ice, or snow. The thermal variation and distribution of water, ice, and snow is dependent on the inherent physical characteristics of the body of water as well as the meteorological conditions at any given time. It is very difficult to accurately describe the thermal and physical parameters of such a scene using direct measurement techniques due to the spatially varying nature of said parameters. Remote broadband thermal mapping approaches offer unique data collection capabilities for this particular environment in that they provide instantaneous spatial coverage of extended areas and capture the varying thermal structure of the scene. However, the sensitivity of a broadband thermal sensor is limited to extracting thermal radiance properties of only the scene's surface and sheds no light on the three-dimensional physical structure below. Given some preliminary knowledge of the physical parameters bounding the observed scene, three-dimensional hydrodynamic models can calculate the energy fluxes at the observed surface and provide estimations for physical parameters, such as water column temperature profiles, ice distribution, and ice thickness. Work is being performed with aims to thermally calibrate an entire water scene in the presence of open water, ice and snow using an aerially-validated, physics-based, hydrodynamic model that has been paired with a genetically-based optimization routine.

The proposed approach uses a genetically-inspired optimization algorithm, particle swarm optimization (PSO), to drive the selection of inputs for a three-dimensional hydrodynamic code, ALGE. ALGE is a computational hydrodynamic code which predicts the movement and dissipation of thermal plumes from any input source (*e.g.* industrial facilities) into bodies of water. Originally, the inputs for ALGE, by definition, included physical parameters which describe the three-dimensional hydrodynamic and thermodynamic states of a body of water and the meteorological conditions at a given time. The outputs from the ALGE model included a surface and volume temperature distribution and a three-dimensional velocity flow map of the given body of water. Recent work has been completed to validate the extension of the ALGE model to generate ice and snow when the water body is in a cold climate. The ice and snow extension added a snow thickness parameter as an additional input into the model. As a result of this extension, the ALGE model now also produces an ice thickness distribution. Sample outputs from the current ice-extended version of the ALGE model are shown below in Figure 3.5.

A large scale, multi-year data campaign was executed in order to accomplish the validation of the ALGE ice and snow extension. These campaigns yielded a database of 13 ground-truthed, calibrated, thermal images of a power plant facility in Midland, MI and provide the empirical data to be used for the optimization functional evaluation. Shown in Figure fig:tempMaps are examples of imagery collected.



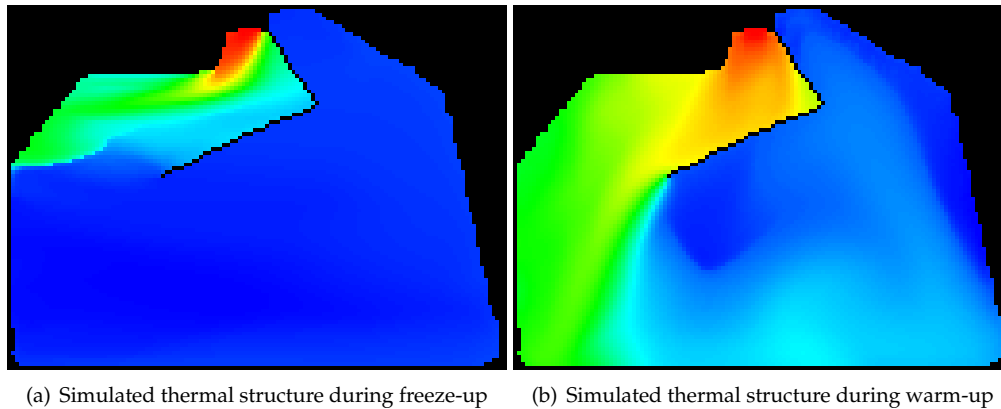


**Figure 3.5-20: ALGE surface temperature predictions for the Midland Cogeneration Venture cooling pond in Midland, MI using historical weather information. Blue indicates colder temperatures and red indicates warmer temperatures. Solid, dark blue areas represent areas covered with well formed ice.**

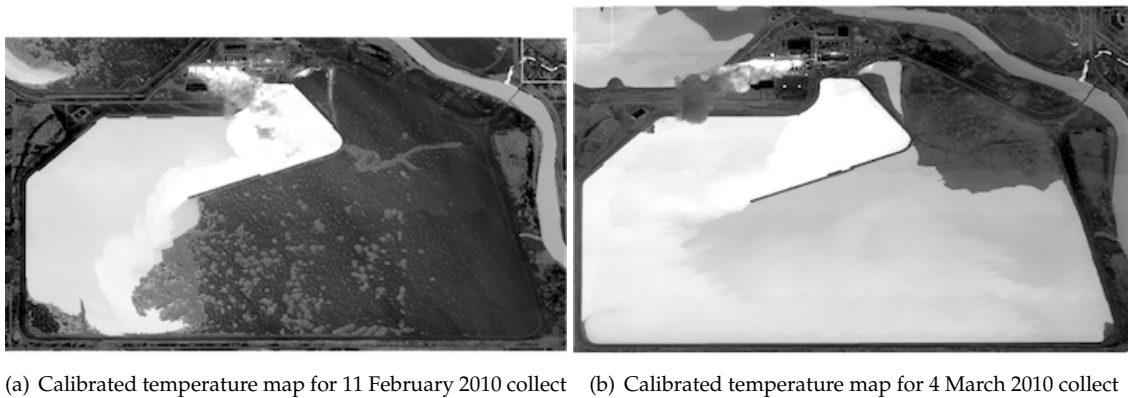


**Figure 3.5-21: Temperature maps created using the implemented calibration technique. NOTE: There is a scale difference between both images.**

Using the Midland, MI facility as the validation site, the goal of this research is to have the PSO algorithm provide the ALGE model inputs to generate both a surface temperature map and an ice thickness distribution which match aerial and empirically collected data within a defined boundary of error. When a model generated by the optimization routine is proven to produce a satisfactory comparison with the collected imagery, the inputs used to create the model will be designated as the real conditions on the ground.

#### Project Status:

The proposed technique will provide a full system-wide optimization and can be employed to model environments where very little is known about ground-based conditions. Additionally, because PSO is a genetic algorithm and evolutionary in nature, only the necessary amount of ALGE simulations will be performed to achieve a defined goal. In comparison to a brute-force technique where every possible ALGE parameter combination is run to create a large look-up table of simulations, a genetic algorithm conserves valuable computational time by only performing simulations necessary until a satisfactory result is achieved. This differing approach has the potential to save hundreds of hours in simulation time to achieve the same results as a traditional look-up table optimization technique.

### 3.6 Small Target Radiometry Restoration

Sponsor: DOE

Principal Investigator(s): Dr. Carl Salvaggio

Research Team: Sarah Paul (CIS - Ph.D.), David Nilosek (CIS - Ph.D.)

Project Description:

Target temperature estimation from thermal infrared (TIR) imagery is a complex task that becomes increasingly more difficult as the target size approaches the size of a projected pixel. At that point the assumption of pixel homogeneity is invalid as the radiance value recorded at the sensor is the result of energy contributions from the target material and any other background material that falls within a pixel boundary. More often than not, thermal infrared pixels are heterogeneous and therefore subpixel temperature extraction becomes an important capability. A typical problem would involve a small, hot target as most objects of interest that exist at elevated temperatures are small dimensioned. Running engines or motors, exhaust plumes from process or manufacturing plants, electrical transformers, individual light sources, and hot water discharges from power plants are just a few examples of these types of targets, all of which are small relative to the footprint of the typical remote sensing systems that are used to monitor them.

A methodology has been developed to retrieve the temperature of an object with a uniform temperature that is smaller than a projected pixel of a single-band TIR image using physics-based modeling. The process is broken into two distinct pieces. In the first part, the Multi-Service Electro-optic Signature (MuSES) thermal signature program in conjunction with the Digital Imaging and Remote Sensing Image Generation (DIRSIG) tool will be used to replicate a collected TIR image based on parameter estimates from the collected image as well as companion high resolution visible imagery of the target. This is done many times to build a multi-dimensional lookup table (LUT). For the second part, a regression model is built from the data in the LUT and is used to perform the temperature retrieval.

The MuSES signature program is the newest addition to the methodology and is currently being integrated into DIRSIG. Previously, DIRSIG lacked the capability to compute the heat transfer via conduction, convection, and thermal radiation between objects in a scene. MuSES is a thermal signature prediction program from ThermoAnalytics and is a voxel-based ray tracer that employs first-principles physics and empirical data to run simulations. For this project, MuSES ingests the geometry of the scene as well as information about the weather, emissivity of the objects, and the heat transfer coefficients for the objects. MuSES then computes a temperature solution based on the environmental and material properties for each facet of the geometry, which results in temperature map of the object. This temperature map is the input to DIRSIG, which then computes the radiance solution. Examples of MuSES temperature solutions can be found in Figure 3.6. In this example, the sun is off the left side of the scene which results in the sun shadow (dark blue area) on the right side of the simulation in Figure 3.6-22(b).

These MuSES simulations were used to help determine the optimum experimental setup to be employed in the collection of real TIR data from the WASP sensor. From these MuSES simulations it was determined that completely filling a container with heater water allows the surface temperature of the object to change with the environment (e.g. wind), but also maintains a uniform surface temperature regardless of if the sun was out. This real-world experiment was executed on 05AUG11 and the data collected has yet to be analyzed.

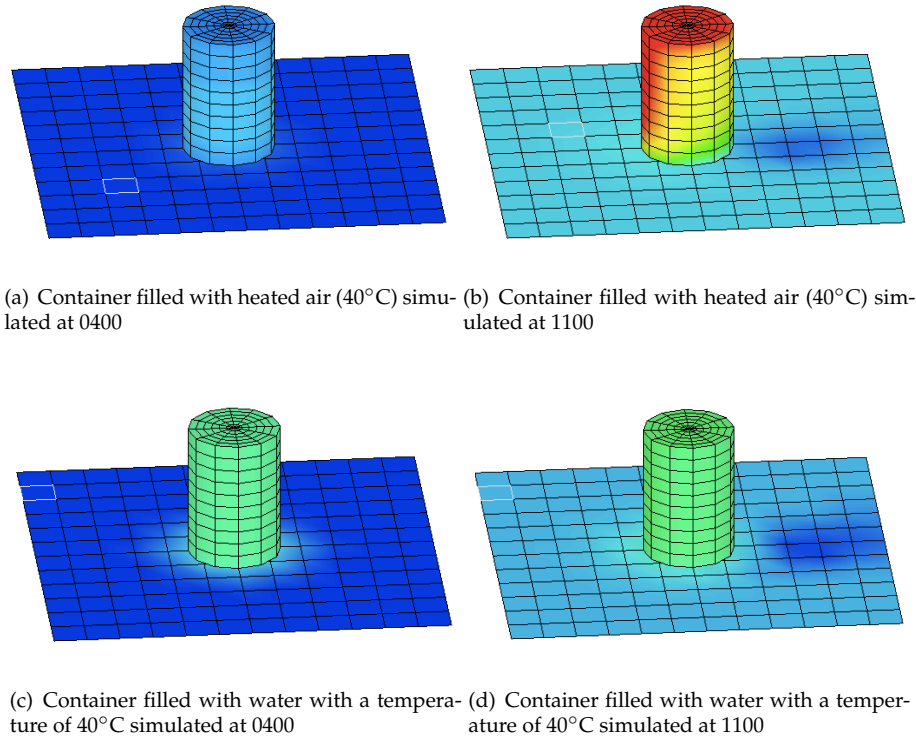


**Figure 3.6-22: MuSES simulations of a metal container on a concrete slab containing air at 40°C [Figures 3.6-22(a) and 3.6-22(b)] and water with a temperature of 40°C [Figures 3.6-22(c) and 3.6-22(d)].**

### 3.7 Analysis of Heavily Laden Vehicles

Sponsor: DOE

Principal Investigator(s): Dr. Carl Salvaggio

Research Team: Troy McKay (CIS - Ph.D.), Jason Faulring, Don McKeown

#### Project Description:

The primary goal of this project is to develop a system of ground-based passive sensors that can be used to accurately determine the weight of large over-the-road vehicles. The first step in the project is to identify multiple vehicle signatures that can be measured remotely from ground-based passive sensors and may have correlation to vehicle weight. The second step is to collect field data using full scale testing for each of the signatures and use the data to quantify the correlation of each signature to vehicle weight. The full scale testing included both a medium size dump truck and full-sized tractor-trailer on closed courses with loads spanning the full range of both vehicle's capacity. The final step is to use statistical analysis and error propagation analysis to develop a method that combines data from multiple heavy vehicle signatures to achieve a more accurate weight measurement than any of the signatures could provide alone.

The following vehicle signatures were chosen as probable indicators of vehicle weight; brake temperature, tire temperature, engine temperature, vehicle acceleration, engine acoustics, vehicle stability, rear differential temperature and tire height. To collect field data on each of the signatures, a system of on-board

and off-board sensors was designed and deployed for two vehicle field tests. The on-board sensing system consists of thermocouples, infrared thermal imagers, triaxial accelerometers, microphones, tire pressure sensors and a global positional system (GPS) receiver. The off-board sensing system consists of the Wildfire Airborne Sensor Program (WASP) infrared sensor system, triaxial accelerometers, microphones and a high definition video camera.

Test plans were developed and executed for two field tests. The first field test was conducted locally and utilized a 1992 Ford F600 flatbed dump truck which had been can be seen in Figure 3.7. The testing consisted of three experiments that were repeated multiple times for vehicle weights of 6, 8, 10 and 12 tons. The first experiment was designed to measure the heat generated by the braking system during a deceleration to a stop from a known velocity over a predetermined distance with the transmission disengaged (clutch in). The second experiment was designed to measure the heat generated by the braking system during a deceleration to a stop from a known velocity over a predetermined distance with the transmission engaged (clutch out). The third experiment was designed to measure the response of the truck's suspension as it travelled over a standard sized speed bump. Data from both the on-board and off-board sensor systems collected data during the entirety of each test runs. The second field test was conducted at the Savannah River Site in South Carolina and utilized the tractor-trailer combination shown in Figure 3.7. The testing consisted of four experiments that were repeated multiple times for loads of 40 tons, 20 tons and 0 tons. The first experiment consisted of accelerating the vehicle to a speed of approximately 35 mph at which point the off-board mounted camera would capture images of the tires. Next, the vehicle would begin braking, during which the WASP sensor would acquire IR imagery. Examples of the imagery acquired by the on-board IR imagers can be seen in Figures 3.7 and 3.7. This experiment was repeated using various braking styles: clutch engaged; clutch disengaged; downshifting; "Jacobs" style exhaust braking. The second experiment called for the vehicle to travel over a set of railroad tracks. The vibration response of the railroad tracks was measured by the two triaxial accelerometers and the pass-by acoustic signal from the vehicle was measured by the two off-road microphones. The third experiment called for the vehicle to accelerate aggressively from a stop while the camera captured video of the front suspension response to the transferring energy. The camera was placed in the center of the road for this experiment with the vehicle traveling directly at it. The fourth experiment required the vehicle to traverse a speed bump at normal speeds while the off-board mounted camera recorded video.

#### Project Status:

The future of this research will involve characterizing the correlation of each of the signatures to vehicle weight using the data collected during the field tests. Ultimately, the goal is to develop a method of combining collected data from each of the valid signatures to provide an accurate vehicle weight measurement.



**Figure 3.7-23: DIRS-owned 1992 Ford F600 flatbed dump truck used for field testing at the Wyoming County International Speedway, Perry, NY.**



Figure 3.7-24: Savannah River National Laboratory furnish tractor trailer used for testing at the Savannah River Site, Aiken, SC.

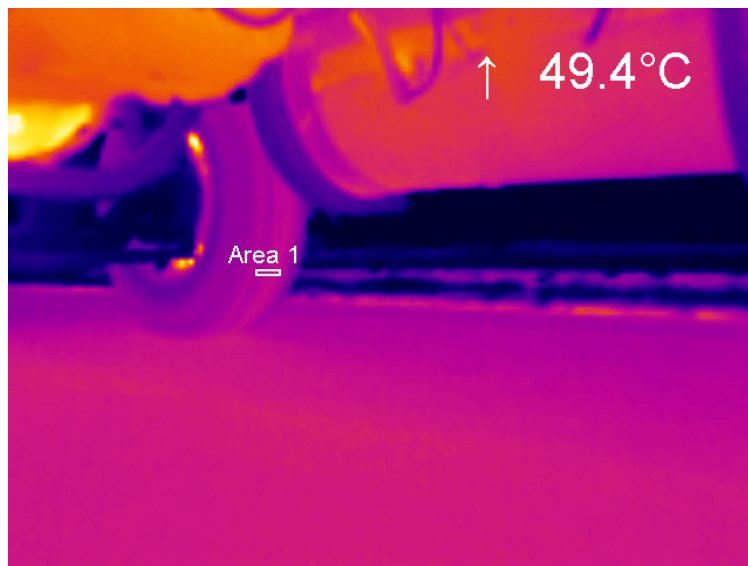


Figure 3.7-25: Front disc brake on Ford F600 flatbed dump truck imaged by on-board MicroEpsilon thermal infrared bolometer camera during field experiment at the Wyoming County International Speedway.

### 3.8 Accurate Radiometric Temperature Measurements using Thermal Infrared Imagery of Small Targets, Physics-Based Modeling, and Companion High-Resolution Optical Image Data Sets

Sponsor: Department of Energy

Principal Investigator(s): Dr. Carl Salvaggio

Research Team: Dr. Rolando Raqueño, Andy Scott, Philip Youkhana (CS - MS)

#### Project Description:

The process of building test scenes to use in simulation-based settings can be a time-consuming and menial task. An ongoing goal of this project is to streamline this process by accepting scene specification via high-level mediums like text input. Conceptually, a user could simply write a paragraph which describes the features and layout of a scene and use a software tool to turn their description into an actual 3-D rendering. However, attempting to process all possible constructs of the english language is infeasible; thus a grammar was crafted which defines a language specific to the context of positioning scene features. A software tool was written to implement the conversion from this language to scene renderings. It also allows the user



**Figure 3.7-26: Rear drum brake on Ford F600 flatbed dump truck imaged by on-board MicroEpsilon thermal infrared bolometer camera during field experiment at the Wyoming County International Speedway.**

to abstract the notion of a scene "feature": A feature may be a single object, a sub-scene, or a grouping of either. This allows for complex feature conceptualization with the sole pre-condition of having access to a set of single-object geometries. With the additional ability to apply a variance scheme to any feature, the tool allows a user to express high-level placement dynamics in smaller terms. Sets of unique renderings can thus be produced from a single specification - automating the process of constructing sets of test sceneries.

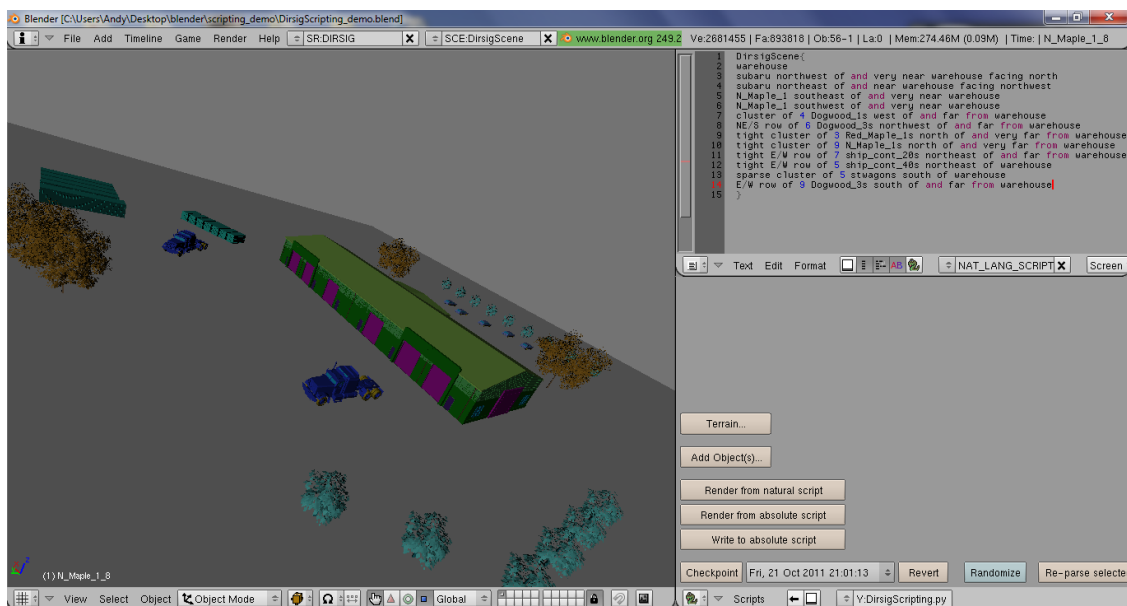


**Figure 3.8-27: Geometry manipulation interface in Blender.**

#### Project Status:

This project has yielded the following results:

- Object geometry protocols established and a preliminary interface/editor designed and implemented
- Two script types for geometry placement have been established and implemented; a clause-based abstracted language and a modeling environment-specific technical script
- A graphical user interface has been implemented in the open-source, platform-independent code Blender to visualize and update technical script (these actions are equivalent)
- A roadmap to use other three-dimensional modeling environments has been established
- Best effort placement of scene elements has been enacted to maintain scene balance if an absolute position is not specified
- Object heading is established during geometry creation and obeys clauses such as facing and compass directions
- Reusable sub-scene clause segment can be cut-and-pasted between separate scenes
- Syntax for object-to-object connectivity has been established and preliminary implementation demonstrated
- Object embedding in and placement of terrains using bounding volumes and Blenders physics engine implemented (including interactive terrain following)
- Developed XML-based schema as a vehicle to build and modify scene descriptions
- Developed & implemented randomization framework identifying and operating on variable aspects of scene features

### **3.9 Lake Kivu Environmental Study**

Sponsor: MacArthur Foundation

Principal Investigator(s): Dr. Tony Vodacek

Research Team: Bikash Basnet (current CIS Ph.D. student). US Collaborators at other universities: Drs. Bob Hecky, Stephanie Guildford, and Sergei Katsev at the University of Minnesota-Duluth, Dr. Cindy Ebinger at the University of Rochester, and Dr. Chris Scholz at the University of Syracuse. Key Rwandan collaborators: Adrie Mukashema at the Centre for GIS and Remote Sensing at the National University of Rwanda, Dr. Antoine Nsabimana at the Kigali Institute of Science and Technology, and Jean Claude Shyirambere at INES-Ruhengeri. Key European collaborators: Drs. Francois Kervyn and Damien Delvaux at the Royal Museum for Central Africa in Belgium and and Dr. Nicolas d'Oreye at the National Museum of Natural History in Luxembourg.

#### Project Description:

Lake Kivu lies at the center and high point of the Albertine Rift, and as such is a focal point for biodiversity in the surrounding montane forests as well as for the fish species in the great lakes of Central and East Africa. A large human population around the lake, including displaced persons, puts growing pressure on the surrounding highland forests for fuel use and subsistence farming, leading to loss of wildlife habitat and increased runoff to and degradation of the nearshore waters of the lake as forests are cleared. Additional risk factors adding to regional environmental stress are the very recent efforts to develop the oil and

methane resources of the Albertine Rift, including the gas-charged waters of Lake Kivu. The result of the largely human-induced stress imposed on both the terrestrial and aquatic environments is added to the inherent, but poorly understood risk imposed by the seismically and volcanically active setting of Lake Kivu within the East African rift system.

This multi-faceted project will 1) systematically acquire seismic reflection, bathymetric, sediment cores, water samples along the length of the lake system; 2) monitor earthquake activity along fault systems and from volcanoes; and 3) analyze time variations in land use and vegetation. Our synergistic approach to surveying this natural system is essential to evaluate the hazards imposed by natural and human activities in the region and to inform the regional governments of the conservation implications of their development efforts in this biologically diverse, unique ecosystem.

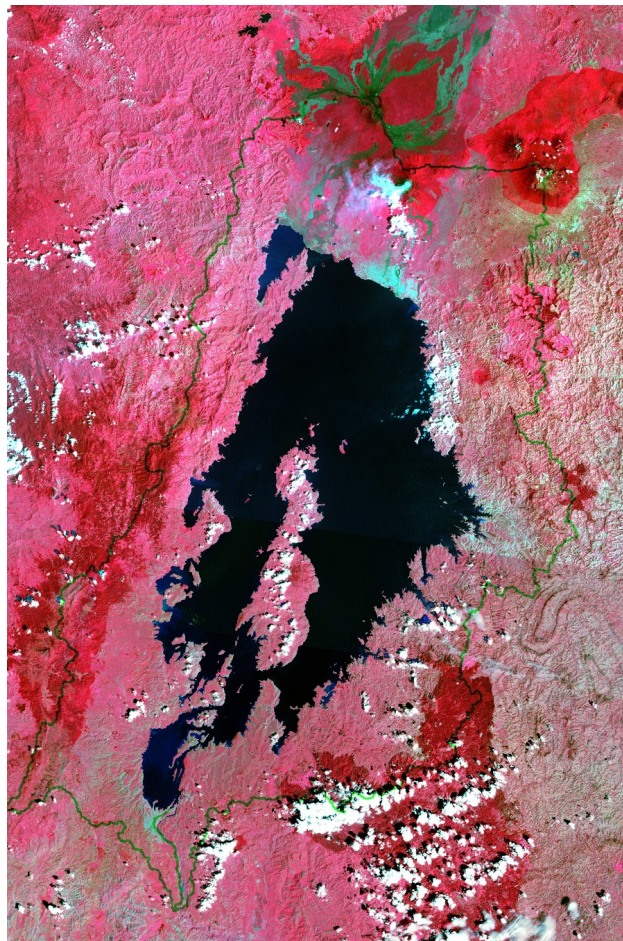


**Figure 3.9-28:** Mosaic of 2 Landsat scenes covering Lake Kivu and its watershed. The watershed is outlined on the image. The Virunga Volcanoes are visible at the top of the image. Lake Kivu drains south through the Rusizi River to Lake Tanganyika.

Project Status:

Preparations are underway for the first of several planned sets of systematic field studies of the lake and its surroundings. Our collaborators will begin survey cruises on the lake by January 2012. Seismometers and GPS installations will occur in spring 2012. Our own work in land cover change analysis using Landsat



data began with the acquisition from the USGS of all existing Landsat images over the study site. We are currently assessing techniques for cloud and cloud shadow screening that will allow us to create pixel-based time series of land cover change for this tropical and mountainous region that experiences frequent cloud cover. Some even earlier image data of the region are available from declassified spy satellite data. To aid in the automated processing of the large amount of image data in this time series we are using the storage and computational assets of the RIT Research Computing group.

### 3.10 Information Products Laboratory for Emergency Response

Sponsor: NSF

Principal Investigator(s): Dr. Jan van Aardt

Research Team: Don McKeown, Steve Cavilia, Jason Faulring, Sanjit Maitra (CIS - Ph.D.), Weihua Sun (CIS - Ph.D.)

Project Description:

The Information Products Laboratory for Emergency Response (IPLER) is a major activity housed within DIRS that seeks to cultivate the application of remote sensing technology and data products within the disaster response community.

IPLER was established in 2009 through a grant from the National Science Foundation (NSF) with a focus on bridging the knowledge gap between remote sensing technology and service providers and information product end users; in essence educating technologists on the needs and constraints of users and educating users on the capabilities of remote sensing technology. IPLER researchers are actively engaged in the development of new information tools and processes that use remotely sensed imagery as a major ingredient. Some of these include

- Automated detection and mapping of temporary shelters (blue tarps)
- Automated building damage assessment
- Automated wildfire mapping
- Delivery of georeferenced multispectral airborne imagery in realtime
- Proof of concept radiological ingestion pathway assessment tool
- Integrated watershed modeling (IPLER partner University at Buffalo)
- Spring runoff flooding analysis (IPLER partner University at Buffalo)
- Post wildfire erosion assessment (IPLER partner University at Buffalo)

Through IPLER, RIT has established partnerships with UB, ImageCat, Kucera International, and the New York State Office of Emergency Management (NYS OEM), among others. These partnerships in particular have been the bridge allowing IPLER to provide support to actual disaster scenarios.

The IPLER support to the World Bank after the Haiti earthquake disaster in 2010 in which high resolution imagery was collected over 250 square miles and immediately disseminated worldwide via the internet, was cited in an April 2011 UN Foundation / Vodaphone Foundation report as having “transformed the response”. Following on the success of the Haiti disaster response for the World Bank in 2010, the IPLER has been very active in 2011 in various exercises and in international and state level emergencies highlighting

the utility of remote sensing-based information to users and providing valuable insight into user needs to technology / service providers.

When the Tugoku earthquake and resulting tsunami struck Japan on March 11, 2011 the International Charter was activated. Working with the US Geological Survey (USGS) Natural Hazards, IPLER joined with ImageCat and a team of other academic institutions to provide map products derived from commercial satellite imagery to emergency managers in Japan.

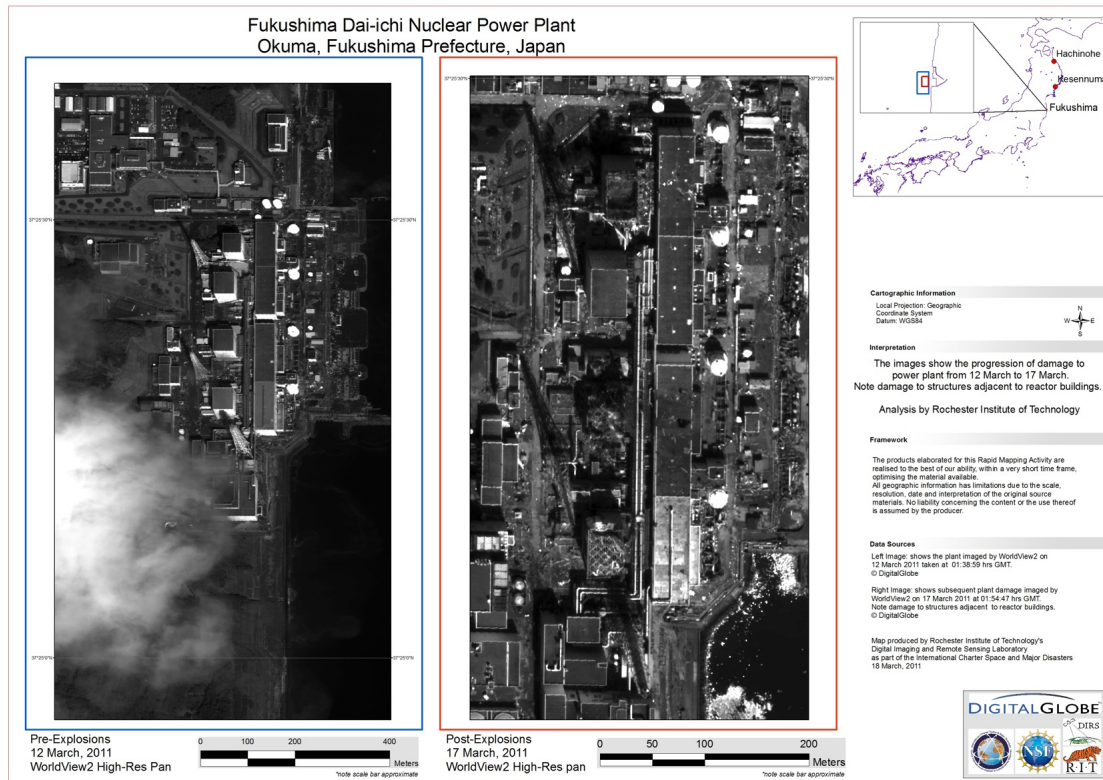


**Figure 3.10-29: IPLER map product showing Fukushima nuclear power plant.**

Specifically, IPLER produced maps for the hard hit areas of Kesennuma, Hachinohe, and the Fukushima nuclear power station. Figure x shows a image map created by IPLER showing the Fukushima plant before and after the explosions there.

As hurricane Irene moved up the east coast in August, IPLER offered to support NYS OEM with imaging of communities along the Schoharie Creek watershed which experienced a 500 year flood as a result of the storm. The offer was accepted and on 28 August, 48 hours after passage of the hurricane/tropical storm, RIT working with Kucera, collected imagery over 28 square miles and began delivery of imagery via ftp server to the NYS OEM within 4 hours after collection. Imagery is being used to plan recovery efforts and to re-evaluate crucial flood models for the area.

A mere week after the Irene flood, the remnants of tropical storm Lee pounded PA and the southern tier of NY with up to 10 inches of rain. The resulting flood greatly exceeded previous records and forced the evacuation of an estimated 100,000 persons in NY and PA. 20,000 were evacuated in the city of Binghamton, NY alone. Again IPLER responded, and with support from NYS OEM and FEMA, executed a rapid aerial map-

ping 23 square miles of the hard hit cities of Binghamton and Johnson City on September 9 approximately eight hours after flood crest. Imagery was available for download 4 hours after collection and a mere 12 hrs after authorization was given to proceed. Flying low, below the cloud layer impervious to satellite imagers, the RIT sensor on the Kucera aircraft collected very high resolution images of the flood in progress. The imagery has been shared with NYS OEM, FEMA, Broome County, and with Energy East, the gas/electric utility responsible for the Binghamton area. Exploitation of the imagery is underway at this time.



**Figure 3.10-30: : Flood waters pour over the Gilboa Dam on Schoharie Creek following rains from Irene. Imagery provided to NYS by IPLER with 4 hours after collection.**

Project Status:

The common thread by which the IPLER PFI succeeds is through the relationships and trust built up between providers like ImageCat and Kucera International, and users such as the USGS, FEMA, and NYS OEM. In a disaster, managers turn to those they trust to understand what they need and who can provide what they want.

IPLER and its partners are continually growing in their understanding of the promise and challenge associated with the use of remote sensing derived information in emergency response.

### **3.11 Modeling Research for Performance-driven Multi-modal Optical Sensors**

Sponsor: Air Force Office of Scientific Research (AFOSR)

Principal Investigator(s): Dr. John Kerekes

Research Team: Michael Presnar (CIS - Ph.D.) Lingfei Meng (CIS - Ph.D.) and Annette Rivas (CIS - M.S.); collaboration with Numerica, Inc., Dayton, Ohio

Project Description:

The objective of this project is to perform basic research in the development and use of integrated micro-



**Figure 3.10-31: Flooded neighborhood in Johnson City, NY. Imagery rapidly collected approximately 8 hours after flood crest.**

electromechanical systems (MEMS) devices coupled with optics and solid state focal plane array technology for adaptive exploitation-driven multi-modality sensing suitable for ISR applications. In particular, we are investigating adaptive sensor designs that enable co-registered electro-optical imagery, video, polarization and spectral sensing in a robust compact unit. These designs are being explored together with research into real-time exploitation algorithms that can adaptively control the sensing modality and field-of-view to enable object tracking and monitoring specific to the situation. These device and algorithm research efforts are being conducted together with scene phenomenology modeling and simulation tools to perform comprehensive system-level performance analyses and demonstrations of the potential for the concepts to lead to transformational ISR capabilities.

Our approach for this effort is to explore feasible optical device constructs which through further research and development could lead to integrated imagery (both intensity and polarization), video and spectroscopic sensing together with the algorithms and scene phenomenology for adaptive sensing and tracking of objects of interest in a cluttered environment. This approach combines three interrelated research veins. 1) Sensor and Device Research. This research thrust is exploring conceptual designs and component modeling for integrated multi-modality optical sensors based on MEMS, digital micromirror, integrated Fabry-Perot, and high resolution lithography technologies. 2) Exploitation Driven Adaptive Sensing. This effort is working on the basic science of algorithms necessary to exploit, track and adaptively control the sensing parameters based on the scene phenomenology, and observational geometry, and target information. 3) System Performance Modeling and Analysis. This third research vein provides the framework using DIRSIG and Matlab for end-to-end system modeling of the device concepts and processing algorithms and enables system level trade-off studies and performance predictions.

#### Project Status:

This year was the third year of the project. Michael Presnar completed his Ph.D. thesis under this project in August 2010. His work demonstrated a full end-to-end modeling capability from a DIRSIG-simulated dynamic scene, through MATLAB sensor models and tracking performance using an enhanced version of Numericas multiple hypothesis tracking algorithm. Annette Rivas completed her MS thesis in August 2011 with a full evaluation of the performance of a single-pixel MEMS Fabry Perot tunable spectrometer. Her

work demonstrated the feasibility (from a modeling perspective) of a device that could rapidly collect data at specific wavelengths. Lingfei Meng continued to make progress in the analysis and modeling of adaptive polarization imaging systems for target detection.

Future work will focus on continuing the optimal integration of spectral, polarimetric, and panchromatic video in the tracking algorithm and estimation of system performance.

### **3.12 Phenomenology Study of Feature Aided Tracking of Dismounts**

Sponsor: Air Force Research Laboratory (AFRL) - Sensors Directorate

Principal Investigator(s): Dr. John Kerekes

Research Team: Jared Herweg (CIS - Ph.D.) and Dr. Emmett Ientilucci

Project Description:

The objective of this project is to investigate the phenomenology sensible by hyperspectral imagers for the purpose of detecting, identifying, and tracking humans in a cluttered environment. The Air Force is interested in this technology as part of combating terrorism and facing the increased challenges of fighting in urban environments.

Project Status:

A successful data collection occurred in June 2011 under this project where hyperspectral imaging and non-imaging data were collected for pedestrians in a typical urban environment. These data will be analyzed to better understand the hyperspectral phenomenology of pedestrians.

### **3.13 Advanced Multi-modal Scene Development**

Sponsor: Raytheon Corporation

Principal Investigator(s): Dr. John Kerekes

Research Team: Chris De Angelis and Dr. Scott Brown

Project Description:

The goal of this project is to develop a highly detailed urban scene in the DIRSIG environment for rendering in multiple modalities including hyperspectral and LIDAR. Starting with the existing MegaScene, additional "neighborhoods" were added including an area with high-rise buildings and a waterfront harbor. Additional details such as street lights, lane markings, power lines, etc. are being added along with enhanced variability in the scene texture.

Project Status:

Much progress has been made with initial renderings expected in late 2011, with the project continuing into 2012.

### **3.14 Model Extraction from Oblique Airborne Imagery (NSF AIR)**

Sponsor: Pictometry, NSF Advanced Innovative Research Program

Principal Investigator(s): Dr. John Kerekes

Research Team: Jie Zhang (CIS - M.S.), Ming Zhang (CIS - M.S.), Nina Raqueño

Project Description:

The goal of this project is to investigate semi-automated methods for the extraction of 3D models of buildings and other objects from the oblique airborne imagery collected by Pictometry. An additional objective is to seek automated methods for the attribution of texture and material identification information for the surfaces of the extracted models.

Project Status:

The project was initiated in May 2011 with the students performing literature reviews.

### 3.15 Enhanced Simulation of Scenarios Through the Incorporation of Process Models

Sponsor: DOE

Principal Investigator(s): Dr. David Messinger

Research Team: Jiangqin Sun (CIS - Ph.D.), Weihua Sun (CIS - Ph.D.)

Project Description:

The objective of this project is to define, develop, implement, and test a methodology for connecting process models to synthetic scene elements for the simulation of temporally varying, observable signatures related to nuclear proliferation activities. These simulations can then be used for algorithm evaluation, sensor design studies, as a hypothesis testing tool for analysis, and a variety of other applications. The Digital Imaging and Remote Sensing Laboratory (DIRS) at the Rochester Institute of Technology has developed the Digital Imaging and Remote Sensing Image Generation (DIRSIG) tool over the past 20+ years to achieve exactly these goals. DIRSIG has a long track record of providing accurate physics-based simulations across several imaging modalities including both the reflective and emissive spectral regimes, polarimetric imaging, and recently, active LIDAR three-dimensional imaging.

The project will build off the technical capabilities of the Digital Imaging and Remote Sensing Image Generation tool (DIRSIG), a physics-based, first-principles radiometric scene simulation tool for generation of synthetic data sets across several modalities (passive reflective and emissive, fully spectral and polarimetric sensors, as well as active, LIDAR systems). These simulations can then be used for algorithm evaluation, sensor design studies, as a hypothesis testing tool for analysis, and a variety of other applications.

The research is defined by two research areas: extraction of features from imagery of existing sites to drive proliferation scenario modeling, and development of the methodology to map the signature impacts of spatial - temporal processes in the DIRSIG scene description.

The spatial - spectral image feature extraction research continues to develop methods to extract relevant features from remotely sensed spectral imagery for use in developing scenes for simulation. These approaches have focused on building footprint extraction and road network identification in cluttered, complex environments.

Recent efforts are focused on proper classification of road pixels and parking lot pixels. After using a flood fill and a size filtering technique, we are able to obtain a relatively noise-free image of the asphalt. Next a graph-based approach is taken to segment the asphalt pixels into logical parts. Salient road segments as well as salient parking lot segments are properly identified by computing the geometric properties of each logical parts. Fig.3.15-32 shows the salient road pixels and the salient parking lot pixels. The next step is to use the connectivity of these logical segments to distinguish the rest of the unclassified asphalt pixels.

The temporal process simulation efforts have started to focus on the overall structure and workflow re-

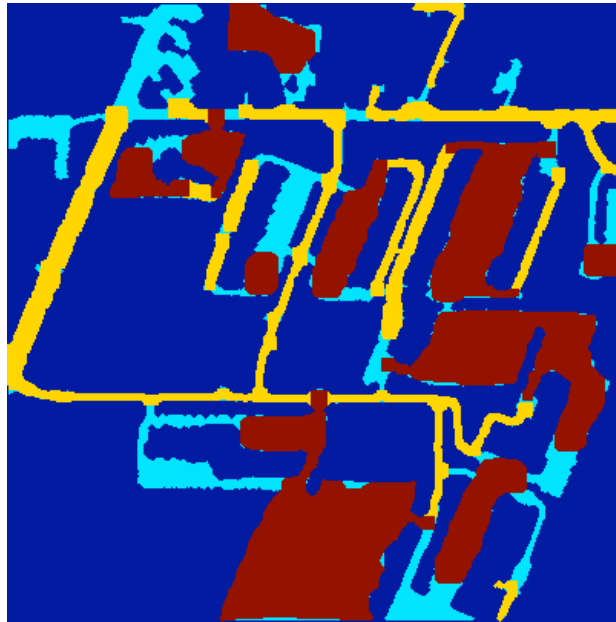


**Figure 3.15-32: Detection of and distinction between roads and parking lots in a Worldview-2 image.**

quired to incorporate external process models into the DIRSIG simulation paradigm. Figure 3.15-33 highlights the current vision of the workflow required. The primary needs of the workflow are the following segments: *standardized output data*, *storage of output data*, and *Data Mapping to DIRSIG files*. The output of the individual process models must be standardized in terms of the input requirements for the DIRSIG simulations. Additionally, a scheme is being developed to store the output data in an efficient and orderly manner. This will be used to access the data as DIRSIG simulations are requested and can also be used as a “truth” output for verification of the resulting simulation signatures. Lastly, the process model outputs must be mapped to the appropriate geometric structures in the DIRSIG simulation inputs.

Project Status:

This project is approximately half completed. Further work on the extraction of features and the automatic inclusion of process models into the DIRSIG workflow will continue, helping to move scene and scenario away from a “brute force” approach.

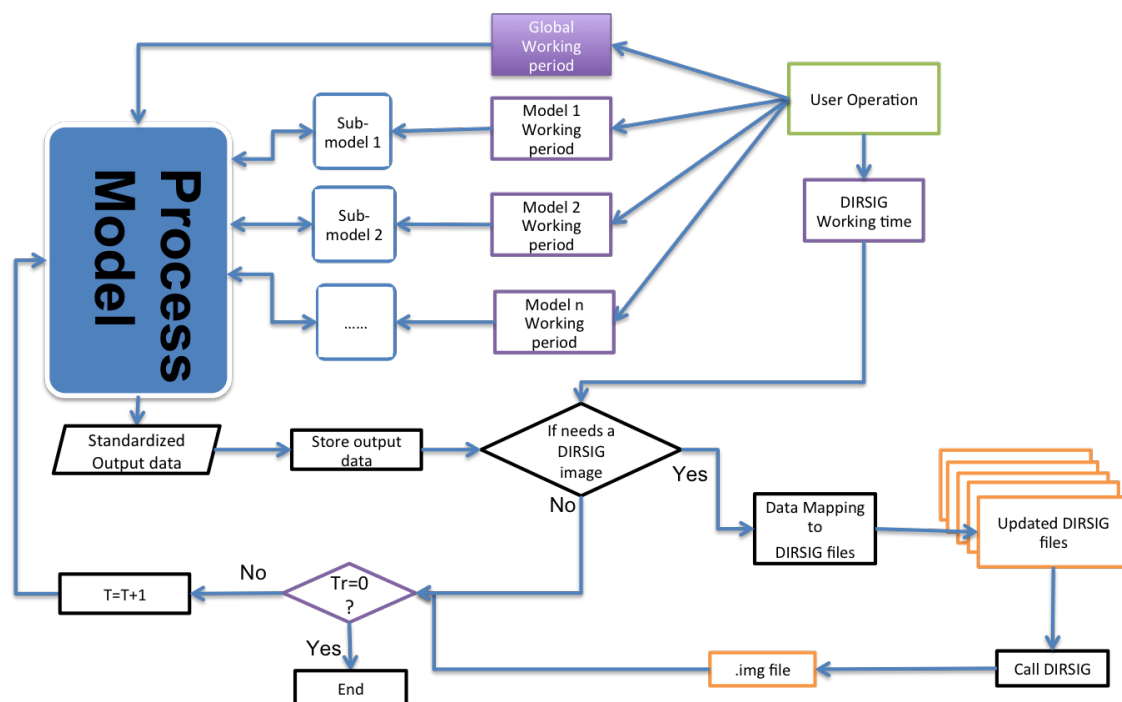


Figure 3.15-33: Workflow describing the incorporation of external process model results into DIRSIG.

### 3.16 Dynamic Analysis of Spectral Imagery

Sponsor: NGA

Principal Investigator(s): Dr. David Messinger

Research Team: Jamie Albano (CIS - Ph.D.), Amanda Ziemann (CIS - Ph.D.)

#### Project Description:

The complex nature of spectral imagery, particularly hyperspectral, necessitates the use of semi-autonomous processing schemes for exploitation. Unfortunately, these methods (typically focused on target or anomaly detection) have proven to be less robust than desirable when applied to large, cluttered scenes. This project presents a novel methodology to use the distribution of the data in the full  $k$  dimensional hyperspace (where  $k$  is the number of spectral bands collected) to identify regions of man-made activity. By identifying such regions for further interrogation, the robustness of the algorithms will be increased and the efficiency of data processing will also be improved. In this way, the hyperspectral imagery is used as a “cue” for further processing, either using the spectral imagery or through other means.

During year three of this NURI Grant we continued the development of the Point Density Approach to hyperspectral image analysis while pushing further into new exploitation methodologies for spectral imagery, all with the intention of identifying regions of “interest” in large area hyperspectral scenes. The Point Density approach seeks to quantify metrics that describe the *distribution* of the pixel data in the hyperspectral space, without levying assumptions on the data (such as multivariate normality, linearity, etc.). During year one, we demonstrated the ability to estimate the correlation dimension of collections of pixels from a hyperspectral image. Previously, the methods used to do this utilized statistical methods such as



Principal Components Analysis (PCA) or Minimum Noise Fraction (MNF). In the Point Density approach, the dimensionality is estimated directly from the data by creating the Point Density Plot (PDP) which describes the rate of change of pixel density in the hyperspace across a distribution of pixels. This method was established and provided insight into the inherent dimensionality of various single material and multiple material clusters in hyperspectral imagery.

Ongoing work is focused on development of the Euclidean Commute Time Distance (ECTD) transformation of the spectral data for use in novel detection algorithms. In this research, the data are represented through the mathematics of a *graph* in the spectral domain. Here, the pixels are the *nodes (or vertices)* of the *graph* and they are connected with *edges* if they fit certain spectral similarity criteria. The ECTD transformation moves the data from the measured spectral domain into a new space where the “distance” between two pixels ( $i$  &  $j$ ) is represented by the estimation of the distance a random walker would have to take to go from pixel  $i$  to pixel  $j$  and back again. Figure 3.16-34 demonstrates the effect of this transformation on synthetic data in two dimensions. After transformation of the data into this new ECTD space, traditional algorithms (such

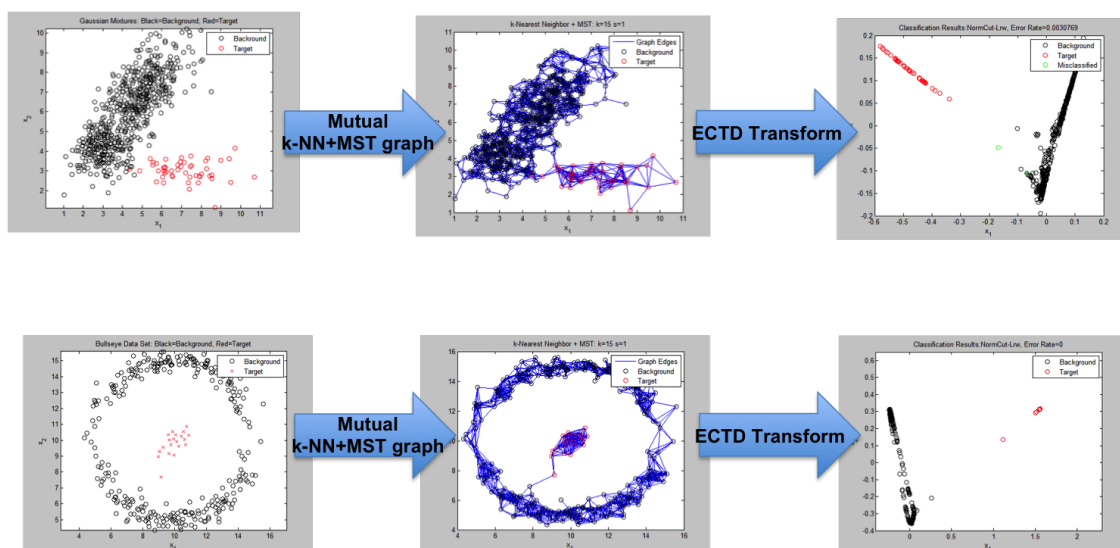


Figure 3.16-34: Examples of the Euclidean Commute Time Distance transformation to 2-D data.

as change detection, anomaly detection, target detection, and clustering) can be performed.

#### Project Status:

This project was extended through the spring of 2012. The ECTD transformation research will seek to use the new data representation to solve difficult image processing challenges. Additionally, novel methods for spectral graph construction are being developed and their impact on the efficacy of processing schemes will be evaluated.

### 3.17 Spatial / Spectral Large Area Search Tool Development

Sponsor: NGA

Principal Investigator(s): Dr. David Messinger

Research Team: Dr. Eli Saber, Abdul Syed (CIS - Ph.D.)

Project Description:

Large area search in imagery for GEOINT targets of interest is a challenging task through means other than visual inspection of pixels. This is largely because it is difficult to identify global mathematical models of the “background” patterns, textures, shapes, colors, etc. This is particularly true when the goal of the search process is to identify not a specific target of interest, but instead when the image analyst is tasked with searching a region for previously unknown targets of interest. These targets can vary in size, shape, texture, signature, etc., and methods designed to identify a particular signature are less than reliable in these circumstances. As an example of the search problem, if an analyst is considering an image that is 15,000 pixels square, they must inspect 225,000,000 pixels. However, if a scheme can reduce the 225 million pixels to something far more manageable (e.g., 225,000, or 22,500 pixels, factors of 1,000 or 10,000) without missing any new targets, this may be acceptable, providing a much more manageable set of regions requiring visual assessment. This research seeks to develop understanding of the spatial and spectral information in multispectral, high-resolution imagery such that it can be exploited to identify regions that deviate from natural backgrounds and thus present themselves as targets for future analysis.

Our strategy to design tools for assisted image interpretation/analysis has a spectral side and a spatial side. Here we highlight work focused on spatial processing of the image. The major tasks involved on the spatial processing can be grouped under the following three areas: Segmentation, Description and Detection. In our initial attempts at solving the problems of Segmentation and Detection, a key issue that surfaced repeatedly is Image Representation. We found it necessary, to include Image Representation as a major subtask of spatial processing. The goal of the representation was to solve the new challenges, not solved by traditional methods. A notional example of the scale space representation is shown in Figure 3.17-35(a). The high resolution image brings with it several challenges. It is highly complex with relevant structures occurring at several scales. A single segmentation or image representation may not capture all the information present in the image and thus requiring multi-scale techniques. A framework for Scale-Space Representation was developed to deal with complexity and organization of multi-scale information. Figure 3.17-35(b) shows the scale-tree of an image from the WorldView-2 Sensor. The scale-tree reflects the scale-space of the image. At the bottom of tree are nodes corresponding to small structures/objects such as cars and ships. Nodes higher in the tree correspond to bigger structures such as roads and buildings.

The scale tree, made up of image regions, does not directly map into an object tree where each node is a semantic object in the scene. The subject of our current research is to improve the scale tree, in the presence of domain or expert knowledge and probabilistic framework, to more closely represent the semantic object structure in the image.

Project Status:

The first option year for this project was granted and the research will continue into 2012. The project will seek to apply these approaches, combined with the spectral processing approaches described in Section 3.16, to large area imagery, particularly imagery from multiple sensors, with varying spatial and spectral resolution, over long periods of time. It is hoped that these methods for transforming and decomposing the imagery will allow for the development of novel analysis and characterization techniques.

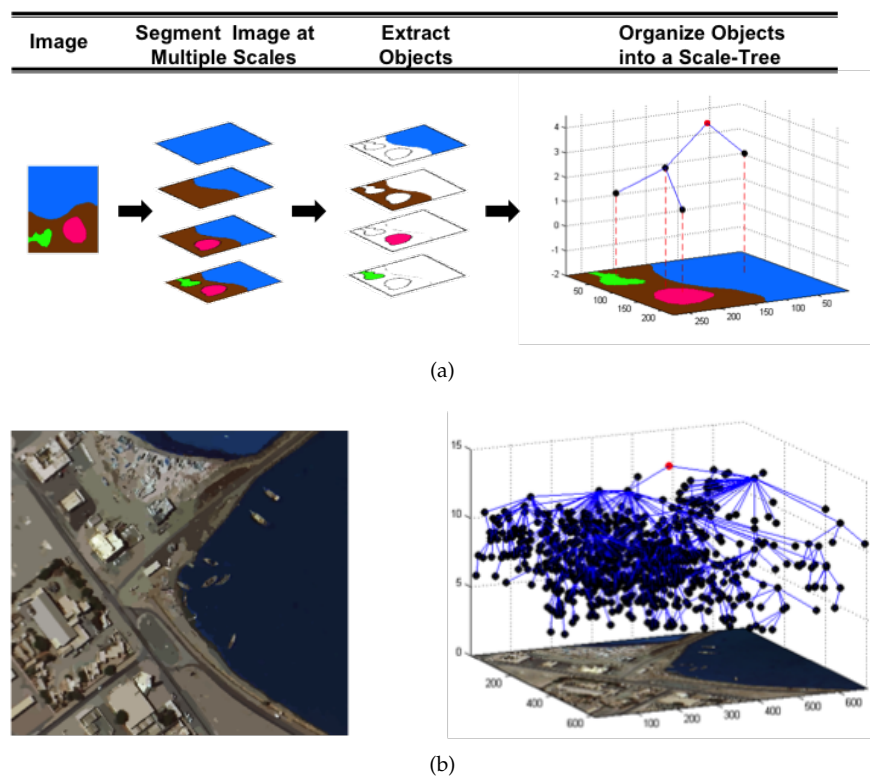


**Figure 3.17-35: Hierarchical scale space tree representations of spectral imagery. (a) Notional image (b) Real image from the Worldview-2 sensor.**

### 3.18 Voxelized Approaches to LIDAR Exploitation

Sponsor: Laboratory for Advanced Spectral Sensing

Principal Investigator(s): Dr. David Messinger

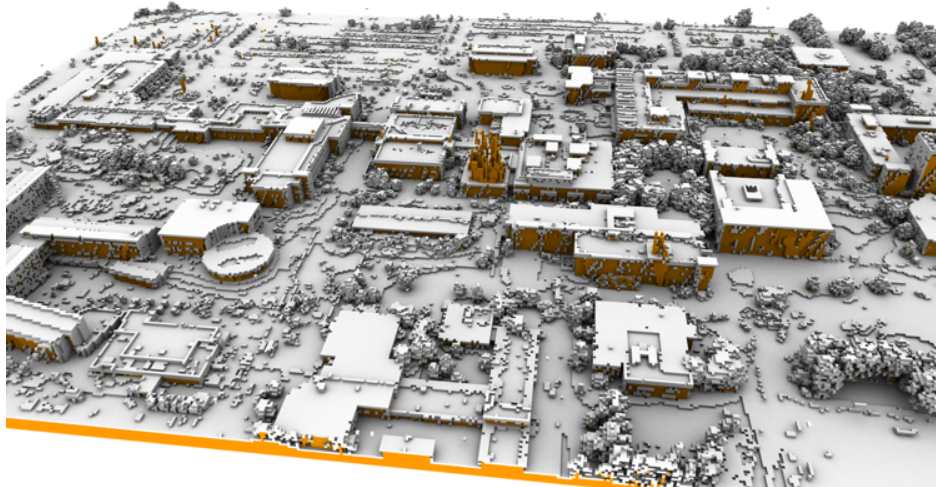
Research Team: Shea Hagstrom (CIS - Ph.D.)

#### Project Description:

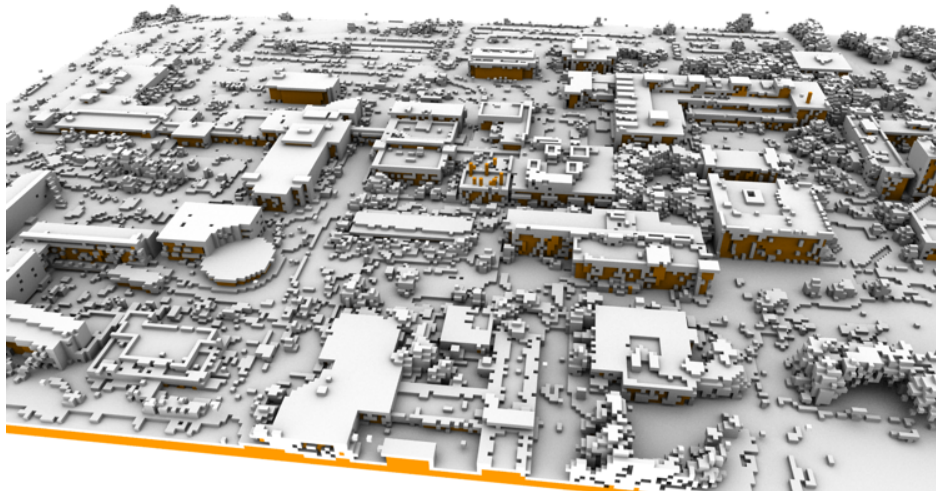
Modern small-footprint LIDAR systems have the ability to resolve structural details at sub-meter sizes, which make them ideal for collecting information to use in line-of-sight analysis. Many existing techniques used to map line-of-sight apply simple surface triangulation to the LIDAR point cloud, but are not well suited to scenes with significant 3D structure and overlapping objects. Newer voxel-based techniques have the ability to describe scene structure accurately, but typically suffer from a lack of information if all scene surfaces are not exhaustively sampled by the LIDAR. LIDAR instrument position is typically discarded after producing the point cloud, but we show how it can be used to identify areas in voxel maps where insufficient data are available. Using this knowledge of under-sampled areas we demonstrate construction of an improved line-of-sight map with metrics that indicate where and why errors in the line-of-sight are likely to occur. During the summer of 2010 an airborne experiment over the RIT campus collected both LIDAR and high resolution visible imagery. The LIDAR point cloud was sampled at several returns per square meter, and the accompanying visible imagery is used to provide context and truth information for LIDAR derived products. A realworld voxel line-of-sight map created from this LIDAR collection is

presented along with an analysis of the associated derived errors.

Figure 3.18-36 shows a voxelized model of the RIT campus derived from multiple flightlines of an airborne LIDAR collection campaign during the summer of 2010.



(a)



(b)

**Figure 3.18-36: Voxelized models of the RIT campus as derived from multiple LIDAR collections (a) 1.25 m voxels (b) 2.0 m voxels.**

This data were used to develop a novel approach to estimating a line-of-sight product (shown in Figure 3.18-37). This new method uses the voxel representation of the data to estimate not only viewable elements of the scene from a given eye-point, but also labels regions that were unsampled as uncertain. This method thus provides a greater sense of knowledge and uncertainty from a particular data collection.

Project Status:

This research is ongoing with the goal of extending this work into the domain of object detection under

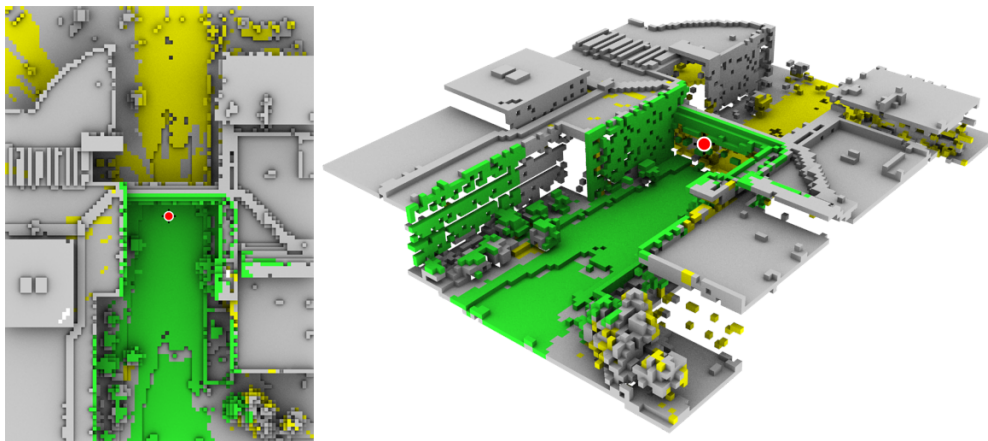


**Figure 3.18-37:** Line of Sight (LOS) map derived from the voxelized LIDAR (1.0 m voxels) representation of the RIT campus. Eye point is near the bridge connecting the Gleason Engineering and Gollisano College buildings (red point). Both nadir looking (left) and oblique (right) views of the viewshed are shown. Green indicates areas that are definitely visible while yellow areas are uncertain.

foliage canopies. Of particular interest is the use of the voxel approach to 3D object change detection.

### 3.19 Remote Sensing for Archeological Studies of Oaxaca, Mexico

Sponsor: NASA ROSES

Principal Investigator(s): Dr. David Messinger, Dr. Bill Middleton (RIT COLA)

Research Team: Kelly Canham (CIS - Ph.D.)

#### Project Description:

Over the past three years, and interdisciplinary team based at the Rochester Institute of Technology (RIT) and the University of Colorado - Boulder (UCB) have been working on the NASA ROSES project “The Hyper- and Multi-spectral Satellite Imagery and the Ecology of State Formation and Complex Societies” We have collected an unprecedented volume of hyper- and multispectral satellite data (primarily from the EO-1 Hyperion and ALI sensors, but also from Quickbird and Worldview-2), as well as geomorphological, paleobotanical, isotopic, and paleoclimatic data from an area of close to 30,000 km<sup>2</sup> in the southern Mexican state of Oaxaca. These data are being utilized to identify and understand patterns of landscape change in relation to the rise and fall of the Zapotec state, one of Ancient Mesoamerica's first state-level societies. One of the tools that archaeologists have used to understand the process of formation of the Zapotec state is full-coverage, regional archaeological survey. As the term implies, full-coverage survey entails the complete coverage of a region, on foot, to identify and assess all surface visible archaeological remains. These data are then used to reconstruct regional settlement patterns, regional population dynamics, regional socioeconomic organization, landscape classification, and how all of this changes over time. Due to the work of many archaeologists over the past three decades, Oaxaca has become one of the most extensively surveyed regions (over 20,000 km<sup>2</sup>) in Mesoamerica and perhaps the world.

The hyperspectral imagery (HSI) collected by the Hyperion sensor onboard the EO-1 satellite has 242 contiguous spectral bands spanning the wavelength range of 0.4  $\mu\text{m}$ -2.5  $\mu\text{m}$ . These sensor parameters provide the capability to identify the number of materials and the materials themselves at the sub-pixel scale. Sub-

pixel image processing is desired because the ground sample distance of the Hyperion sensor is 30m, which is on the same size or larger than most physical and archaeological features of interest in this study. Additionally, the environmental landscape of the 30,000 km<sup>2</sup> collection area in Oaxaca, Mexico, contains over 13 recognized ecosystem classifications. Due to all of these requirements and limitations, spectral unmixing and spectral feature indexes have shown the most success for determining the sub-pixel materials found within the Hyperion data. Past work has focused on the development of spectral tools which can produce abundance or classification maps of the Hyperion imagery and identifying the number of materials present in the dataset in a non-subjective manner.

Spatial and spectral information must be carefully considered when working with the Oaxaca Hyperion dataset because of the large coverage size and the ecological diversity found within a single Hyperion scene. Spectral unmixing is a method to find the amount or abundance of a series of materials/endmembers from within a single pixel. The Spatially Adaptive Spectral Unmixing methodology, developed under this effort, is a modular algorithm which in its current configuration takes advantage of the spatially local image complexity score and a data dimensionality estimator to predict the number of unique materials present in the imagery automatically. The Spatially Adaptive Spectral Unmixing methodology also has shown interesting unmixing results when applied to multi-spectral high-resolution imagery from the WorldView-2 sensor. This unmixing methodology can be applied to the MSI datasets because it unmixes at the local tile level where the band-number-constraint does not impact the number of materials estimated for small tile sizes. However, both of these unmixing methodologies only find the abundance maps for the endmembers identified. An example of this spatially adaptive approach, as applied to the multispectral Worldview-2 image of Oaxaca, Mexico, is shown in Figure 3.19-38. Here, the image has been decomposed into 5 material classes + 1 noise class. These material classifications highlight the differences between land use over large areas.

During this research project, Ms. Canham has received two prestigious awards based on her research. Her algorithmic approach to spatially adaptive spectral unmixing of multispectral imagery won the "8-Band Challenge", and international competition sponsored by DigitalGlobe, Inc., builders and operators of the Worldview-2 platform. Additionally, she was awarded an Alexander Goetz award from Applied Spectral Devices (ASD) to perform ground truth in Oaxaca, Mexico. For that, she has been granted the use of ASD FieldSpec Pro field spectrometer to aid in her research.

#### Project Status:

This project is ongoing. Kelly Canham and Dr. Middleton will be traveling to Oaxaca, Mexico in December 2011 to conduct ground truth experiments to aid in the validation of the spectral unmixing results.

### **3.20 Geometrically Constrained Signature Spaces for Physics-Based Material Detection**

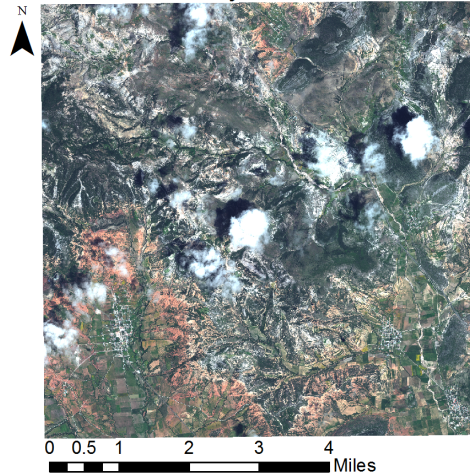
Sponsor: ITT Geospatial Systems and the NGA

Principal Investigator(s): Dr. Emmett Ientilucci

#### Project Description:

The goal of this project is to develop new algorithms and methods that combine information from hyperspectral and LIDAR data to better identify objects of interest. The hyperspectral data enables one to better understand the material properties of an object. The LIDAR data enables one to define the dimensions and shape of an object. Spatial techniques will be used, collectively with HSI and a technique of constrained target spaces, to further enhance material detection by mitigating false alarms based on shape rather than spectral character. This leveraging of LIDAR data is to be bundled in a user friendly software environment.

True-Color WorldView-2 Satellite Image of  
Yanhuitlan Valley in Oaxaca, Mexico



Unmixed Classification Map of  
Yanhuitlan Valley in Oaxaca, Mexico

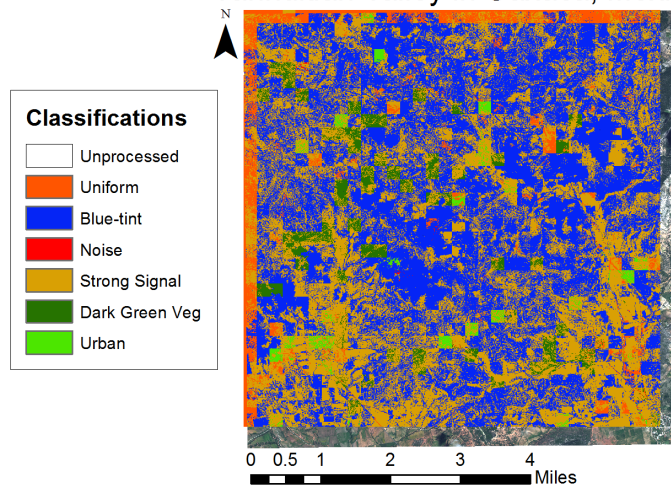


Figure 3.19-38: Example result from applying the LoGlo approach to spectral unmixing to Worldview-2 imagery over Oaxaca, Mexico.

#### Project Status:

This first year effort focused on the development of algorithms that could process LIDAR (co-registered with HSI (data to produce per-pixel maps related to shadow, shape factor (*i.e.*, how much of sky a pixel sees) and terrain angle. Example maps can be see in Figure 3.20-39. These maps are to be used in an ENVI plug-in GUI as illustrated in Figure 3.20-40. This software is capable of ingesting HSI and LIDAR maps. The user then selects a method of detection followed by some optional output parameters. Results are displayed to the use within the ENVI environment.

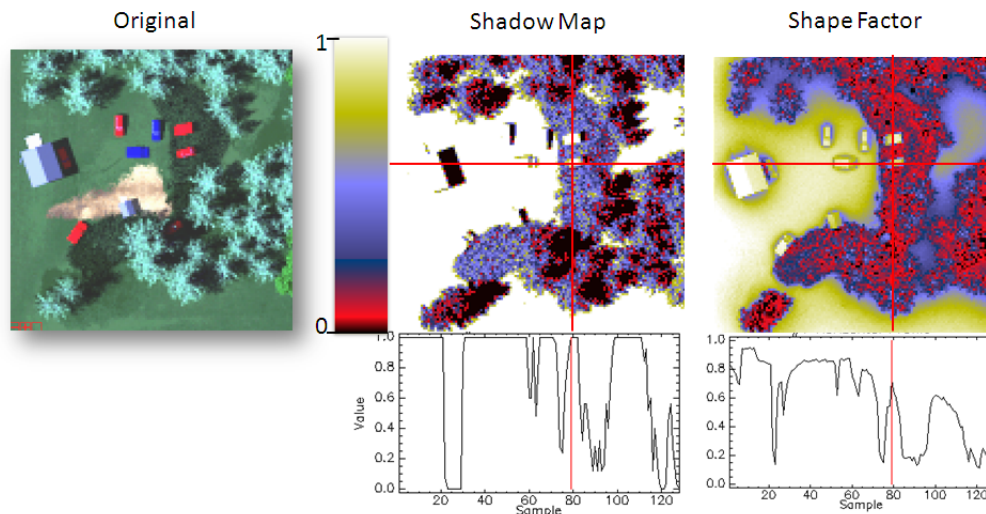


Figure 3.20-39: Sample b) shadow and c) shape factor maps relative to the a) original HSI image.

### 3.21 Passive Infrared Detection of Aerosol Spores

Sponsor: deciBel Research Incorporated through Army STTR

Principal Investigator(s): Dr. Emmett Ientilucci

#### Project Description:

The US Joint Services have the need for a small, lightweight, inexpensive sensor for standoff detection and tracking of biological aerosols. It has recently been shown that aerosolized bacterial spores possess a strong infrared signature that can be detected by passive infrared sensors for detection and tracking of the aerosol plume. The goal of the research (executed by dB and RIT) is to develop a passive infrared standoff sensor that is optimized for the detection, identification, and tracking of biological aerosols.

RIT brings direct experience to this problem via an understanding of Mie scattering theory and spectral-polarimetric radiometric modeling. RIT conducted research into determining representative bio-aerosol signature profiles in the MWIR and LWIR region of the spectrum. Additionally, RIT built a radiometric framework for estimating the magnitude of the Mie scattering signatures under a variety of atmospheric conditions and bio-aerosol cloud sizes. This framework leverages existing Mie scattering theory and utilize state of the art atmospheric radiation transport models, such as MODTRAN.

#### Project Status:

The goal of the project was to develop a radiometric polarized model framework that could estimate a MWIR/LWIR signature (i.e., 3.5 to 14  $\mu\text{m}$ ), as seen by an observer, from a bio-aerosol cloud. The overall layout of a scenario for the model can be seen in Figure 3.21-41. The polarimetric model developed utilized input from both an RIT developed/modified polarized Mie scattering code and the atmospheric radiation propagation model, MODTRAN. The model was successfully cross-validated against a similar published model (i.e., similar end result but different approach) by Avishai Ben-David, et. al.

We then analyzed how the signatures would change by varying the clouds number density, size, surround-



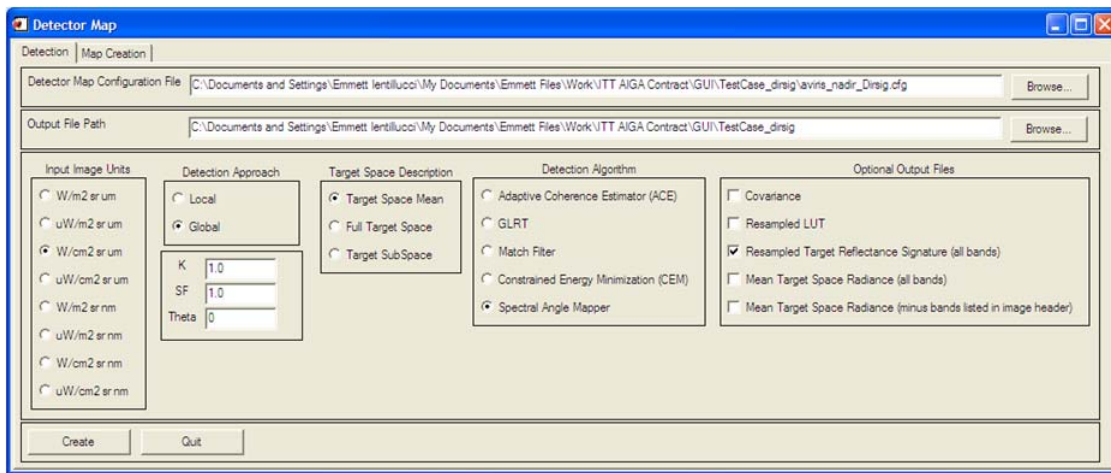


Figure 3.20-40: Screen grab of current version of HSI/LIDAR target detection software tool.

ing atmosphere, and background object type (e.g., blackbody mountain). The coldest/driest atmosphere produced the lowest magnitude radiance signatures while that of a tropical environment exhibited overall larger magnitude curves with a more difficult ability to discern having a mountain in the background versus just open sky. The number density was altered from 10,000 to 50,000 ACPLA. The increase in the magnitude of the radiance contrast (i.e., cloud versus no cloud) seemed to linear increase with number density. The bio-aerosol cloud size was also varied from 100 to 300 meters (see Figure 3.21-42). Here too, the magnitude of the radiance contrast seemed to increase somewhat linearly with an increase in cloud size (more specifically volume).

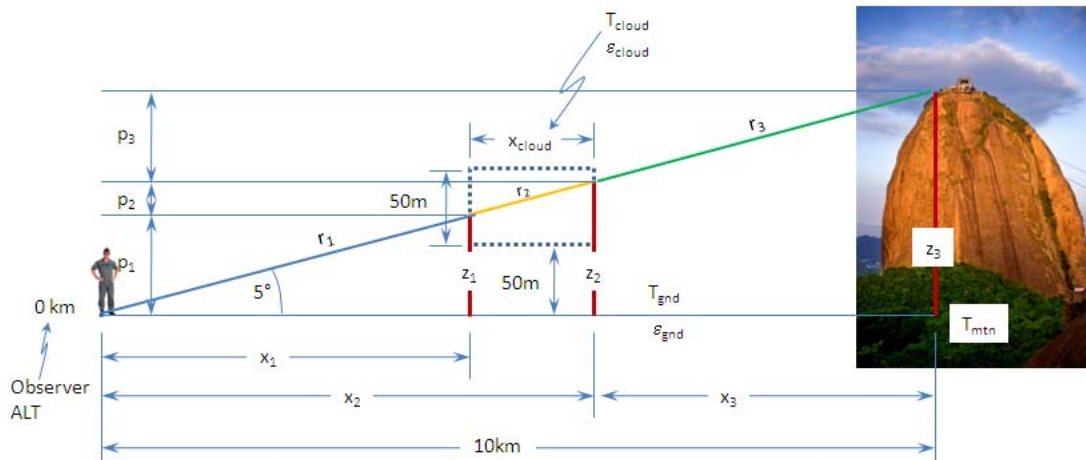
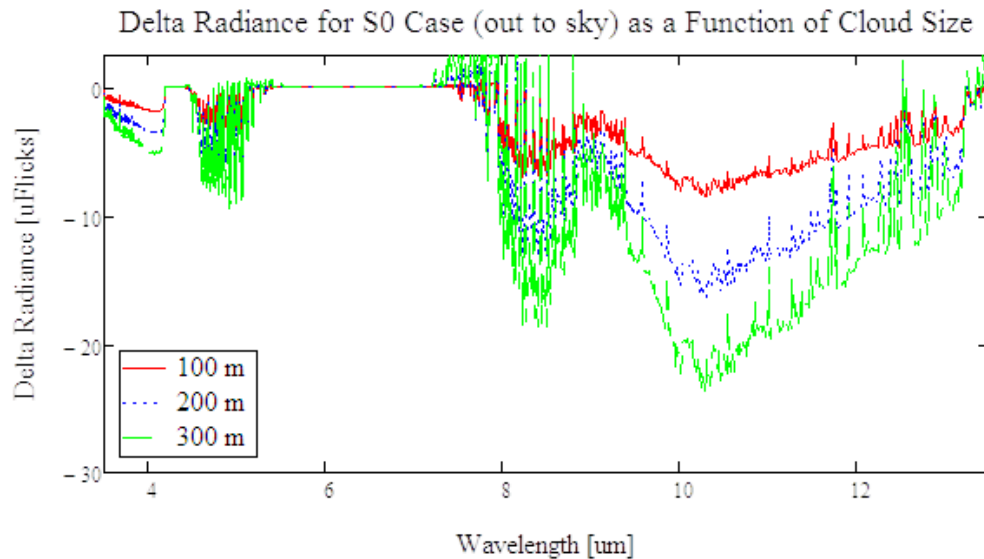


Figure 3.21-41: Overall scene layout illustrating an aerosolized cloud with a potential object in background.



**Figure 3.21-42:** Delta radiance curves for the particular case of  $S_0$  with no mountain in the background (i.e., just sky) for three different cloud sizes. ACPLA was 25,000 using the US 1976 Standard atmosphere. The units  $\mu\text{Flicks} = 10E^{-6} [W cm^{-2} sr^{-1} cm]$ .

### 3.22 Modeling a Polarized LIDAR System with DIRSIG

Sponsor: System Dynamics International through Army STTR

Principal Investigator(s): Dr. Emmett Ientilucci

#### Project Description:

RIT's DIRSIG model is built on a framework of objects that provide the bookkeeping to simulate the spatial, spectral, temporal and polarimetric distribution of radiation in a scene. This framework is backed by a flexible set of instrument models that collect this radiation. In the case of the active LASER modalities (LIDAR and LADAR), the instrument actively illuminates the scene and collects the reflected radiation using a bi-directional propagation method that can compute higher order bounces in a computationally efficient manner. In addition, the returns onto the LIDAR receiver include the passive contributions of reflected and scattered energy from the sun, moon, sky, etc. Unlike other models that leverage raster oriented methods (compute range and intensity across an entire scene), the DIRSIG model simulates the data collection including the LASER pulse shape, LASER transverse beam profile, pulse rate, platform motion, platform-relative scanning, knowledge errors and uncertainty, etc. to produce point clouds using the similar data formation pipelines used in real hardware. These point clouds can be rastered into image products using existing exploitation tools. An overview of what is considered during a passive LIDAR DIRSIG simulation can be seen in Figure 3.22-43.

The DIRSIG model has already been demonstrated to model passive polarized systems using a combination of polarized illumination (MODTRAN4-P), polarized scene optical properties (pBRDFs) and polarization sensitive receivers. To date, all LIDAR simulation work has assumed an un-polarized LASER source and a non-selective receiver. The objective of this study was to investigate how to model a polarized LIDAR system with DIRSIG. This will include the investigation of methods to include polarized LASER source

models, correctly compute the primary and higher order returns from objects in the scene and define polarized receiver descriptions.

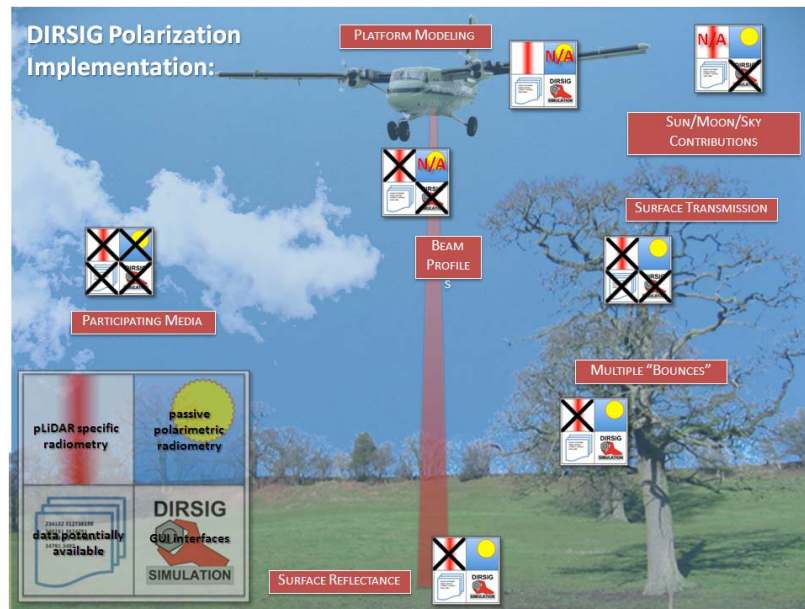


Figure 3.22-43: Simplified overview of what is considered during a passive LIDAR DIRSIG run.

#### Project Status:

To address some of the limitations stated previously, the core mechanics of DIRSIG have been re-written to provide a faster, streamlined storage object (resulting in an order of magnitude speed increase at runtime for all LIDAR runs) and now natively supports spectral Stokes vector gate data under a polarized simulation and spectral scalar data otherwise. Beyond the core radiometry routines, we (RIT) are implementing the prototype pLIDAR beams via a polarizing filter analogue, exploiting existing (unpolarized) source models and inputs by virtually polarizing the beam as it leaves the source. Beyond that, we will be transferring over existing polarimetric tools for surface interactions to facilitate direct (i.e. no multiple scattering) solutions for the prototype and will be outputting the gated data in a format similar to the existing unpolarized data.

### 3.23 Improved Plume Simulation in DIRSIG

Sponsor: Spectral Sciences, Inc.

Principle Investigator(s): Dr. Scott Brown

Research Team: Dr. Adam Goodenough and Erin Ontiveros

Project Description: Spectral Sciences, Inc. is the developer of the widely-used MODTRAN atmospheric radiative transfer model. For this project, they had a Phase II SBIR contract to continue to work on an “embedded plume” feature in MODTRAN5. The feature allows the user to specify an atmosphere and then specify a profile of gas temperatures and concentrations along the path defined for the specific MODTRAN run. Since DIRSIG already had an implementation of a plume model described by Alfred Blackadar in his book “Turbulence and Diffusion in the Atmosphere”, we were able to team up with them to show how this MODTRAN5 feature could be used by other software.

The Blackadar plume model uses a temporally correlated turbulence representation of the atmosphere and a steady stream of small puffs that blow downwind and expand. A example series of images of the plume over time is shown in Figure 3.23-44.

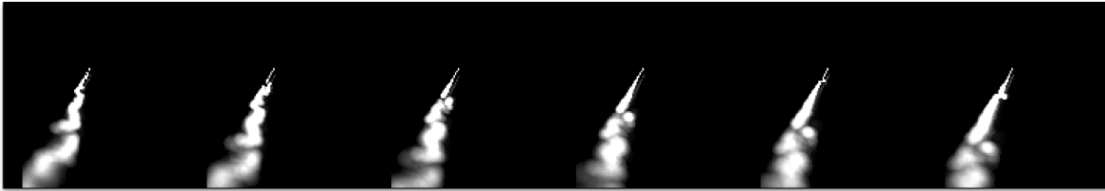


**Figure 3.23-44: A series of images of a meandering plume generated using the Blackadar model over time.**

The plot in Figure 3.23-45 visualizes the average temperature of parallel sampling paths through the plume. During a DIRSIG simulation, lines-of-sight are generated based on the described sensor as a function of time. During a simulation, each pixel is sampled using a set of rays to capture the sub-pixel variability, and these rays are cast into the scene. If a rays intersects the plume, then the temperature and concentration profile along the ray is extracted for processing by the radiometry model. Since multiple instances of the plume model might be present in the scene, overlapping plumes are possible. The DIRSIG model will create individual profiles for each plume, but the profiles are combined in the radiometry model to produce the effect of mixed plumes. Note that there are no mechanisms to model additional chemistry that may result from the plumes mixing.

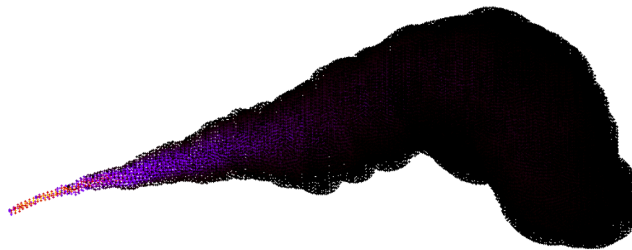


**Figure 3.23-45: A visualization of plume temperatures.**

Project Status: One of the things we take pride in with DIRSIG is that the software architecture is very modular. In the case of radiometry, the user has the ability to choose radiometry algorithms (or what we call *radiometry solvers*) on a per-material basis. This means we can have a suite of algorithms for similar problems or specialized algorithms for specific problems. In the case of plume radiometry, DIRSIG already had a solver specialized radiometry solver for emissive/absorptive volumes. To incorporate this enhanced version of MODTRAN5, we simply created a new solver that converted the profile of gas temperatures and concentrations into the MODTRAN inputs, ran MODTRAN and then read the results back into DIRSIG to be combined with the other radiometric contributors for that line-of-sight. This basic flow is illustrated in Figure 3.23-46.

The plot in Figure 3.23-47 shows an example spectral radiance of a pixel with and without a plume present in it. The radiance curve with the plume present is a combination of the standard DIRSIG radiometry and the radiometry of the plume as computed by MODTRAN5.

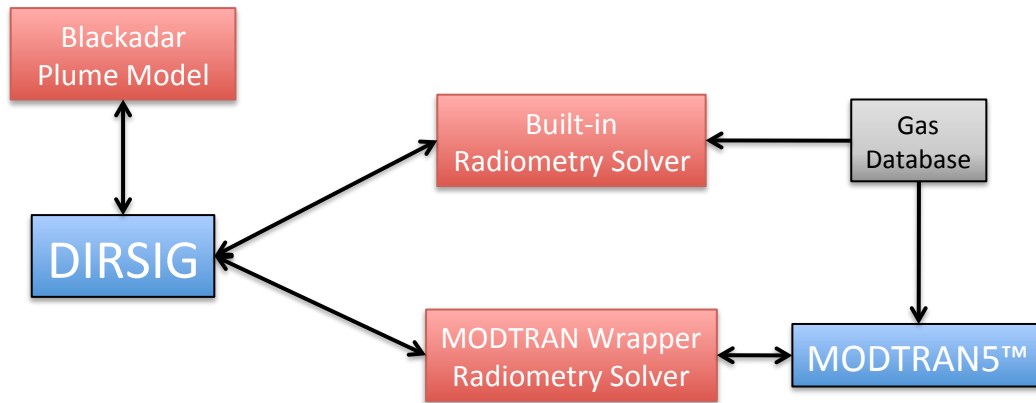


Figure 3.23-46: A flowchart of the way DIRSIG integrates different back-end radiometry solutions for the temperature and concentrations predicted by the Blackadar Plume model.

### 3.24 3D Model Extraction and Representation

Sponsor: Esri

Principal Investigator(s): Dr. Scott Brown

Research Team: Carl Salvaggio, Harvey Rhody, Mike Richardson, Nina Raqueno, Robert Krzaczek, Erin Ontiveros and David Nilosek (CIS - Ph.D.)

#### Project Description:

Ultimately, the goal of this research area is the creation of physically attributed, 3D models of a site that could be explored, visualized and rendered by multi-model modeling tools like DIRSIG. In operation, the user will jumpstart a site model by dumping a set of multi-model imagery into the RIT image geometry toolbox. This may include pan, MSI, HSI, PI, etc. imagery. It may or may not include information about sensor models and platform ephemeris. The toolset will generate a 3D model of the site. That site model will be comprised of 3D polygonal data (fall back to simple 2D geo-projection if we only have 1 image). The various image modalities will be used to derive physical properties for the surfaces of these geometry models. These descriptions will allow the site model to be simulated in a variety of modalities. As the lifetime of a site model evolves, more image data will be added to the site database. New data can be used by the toolchain to refine the site model. The underlying toolbox might be able to identify if the new data fills data gaps or if it duplicates existing data but provides contradictory information. In the later case, that might be flagged as a change in the scene. As part of the capability, it is desirable to be able to identify gaps in the data that might be filled by future collections.

The overall goal is to leverage the wealth of image geometry algorithms to create 3D site models from collections of 2D images that are back-ended by physics descriptions. The toolbox of algorithms we are using contain 2D to 2D (image to image), 2D to 3D (image to model) and 3D to 3D (model to model) tools. These tools have been combined in a toolchain to perform relative registration of data, 3D model creation and 2D to 3D model mappings. Most of our work has leveraged the “photo-tourism” techniques developed by Dr. Noah Snavely at the University at Washington. His general approach is called “structure from motion” (SfM) and is based using large collections of images of the same site (usually collected by tourist) and identifying registering the images together in a 3D space through the a combination of image feature extraction, feature matching and 3D object space reconstruction. The work at RIT has largely focused on

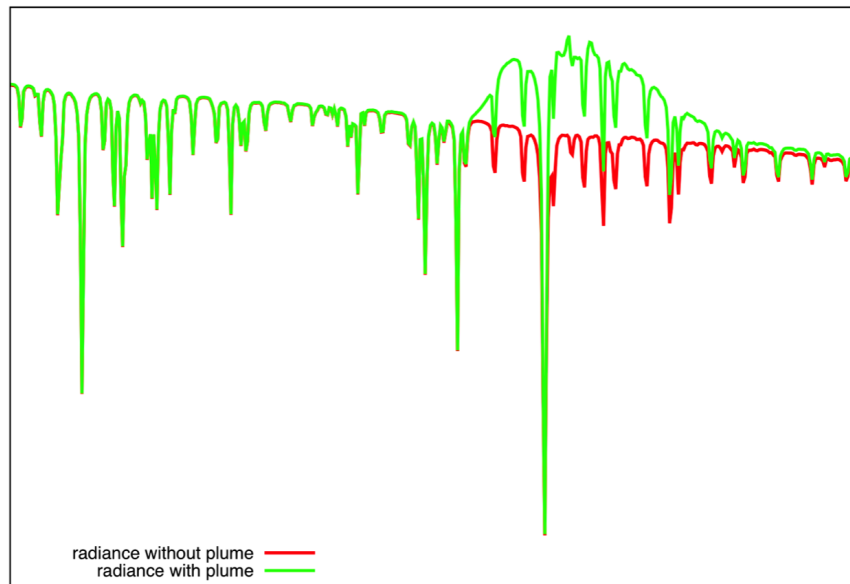


**Figure 3.23-47: A plot of a pixel with and without the plume.**

how these approaches can be applied to overhead imagery which is generally characterized by lower spatial resolution and decreased image coverage (fewer images of the same site). A summary of the algorithm workflow is illustrated in Figure 3.24-48.

#### Project Status:

During the last year, David Nilosek (Ph.D.) has been working on the refinements to a semi-automated Structure From Motion workflow to process overhead, remotely sensed imagery. The rest of the team has focused on the porting of these tools to an environment that allows the approach to be more easily integrated with the tools produced by Esri. During the upcoming year, David Nilosek's work will increasingly focus on the extraction of 3D structures (polygons) from dense point clouds.

The team has also conducted several studies to explore the robustness of these tools with different datasets. Figure 3.24-49 shows the projected footprints of 14 images collected by the RIT WASP sensor of the RIT campus. Various combinations of images were feed to the tools to generated point clouds for analysis. The goals of this analysis is identify image selection criteria that can be automated to produce the "best" point clouds. The definition of "best" is another active area of research, and several metrics addressing point accuracy, point density and point uniformity have been proposed and explored. An example dense point produced using the RIT imagery is displayed in Figure 3.24-50.

### **3.25 DIRSIG Infrastructure**

Sponsor: Internally Funded

Principle Investigator(s): Scott Brown

Research Team: Scott Brown, Niek Sanders, Mike Gartley and Adam Goodenough

Project Description:

In addition to the sponsored research projects that address the enhancement of the DIRSIG model, RIT has

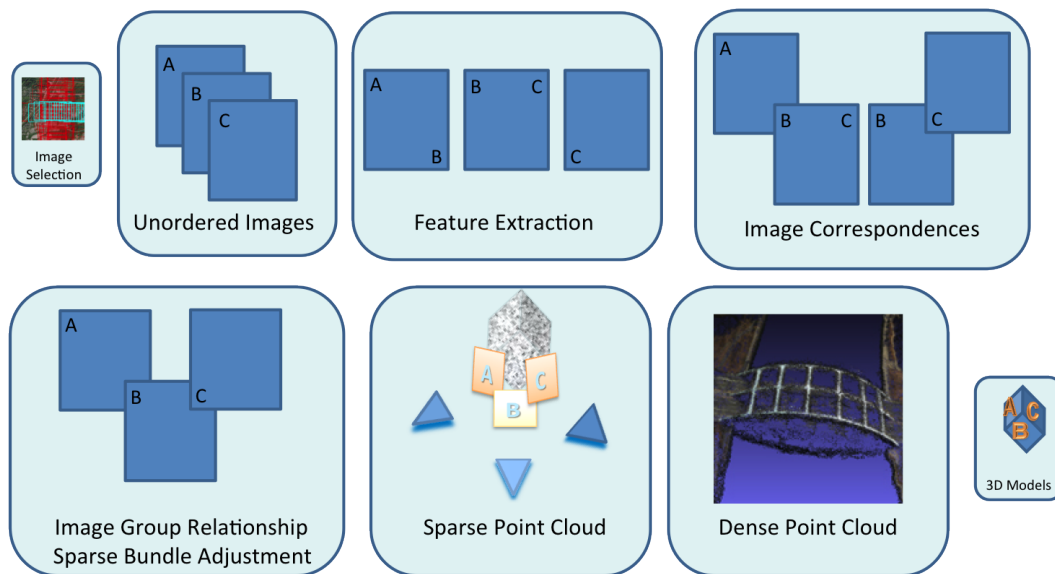


**Figure 3.24-48: Flowchart of the general “structure from motion” workflow adapted for overhead, remotely sensed imagery.**

been slowly increasing the amount of internally funded staff time that is spent working on infra-structural DIRSIG development. We internally fund a great deal of the strategic software development that allows us to accomplish research already in-house and compete for new research opportunities. One of the fundamental funding streams for DIRSIG core development has been the DIRSIG Training Courses, which was offered on four (4) different occasions during the last calendar year, including off-site sessions in Fairfax VA, Herndon VA and Mountain View CA.

The goal of this ongoing project is the continued improvement of the DIRSIG user experience. Specifically, to improve the utility of the tool and integration of the tool with other engineering tools commonly used alongside DIRSIG.

#### Project Status:

During most of the past year, the development team focused on Release 4.4. The important milestones of that effort was the continued improvements to the graphical user interface (GUI) in an effort to make the GUI an invaluable tool to new and old users. The following list highlights the new features introduced in the 4.4 release.

- A optimization involving dynamic scene geometry that significantly improved run-times for scenes with large numbers of moving objects (for example, scenes containing SUMO predicted traffic patterns).
- The introduction of the “platform data recorder” instrument, which can be used to record the location and orientation of the platform during a simulated collection.
- Improved support for the Alias/Wavefront OBJ geometry format to utilize vertex normals and texture vertexes.
- Improvements to the user-interfaces for the MODTRAN-driven atmospheres to simplify the ability of users to provide customized MODTRAN configurations.

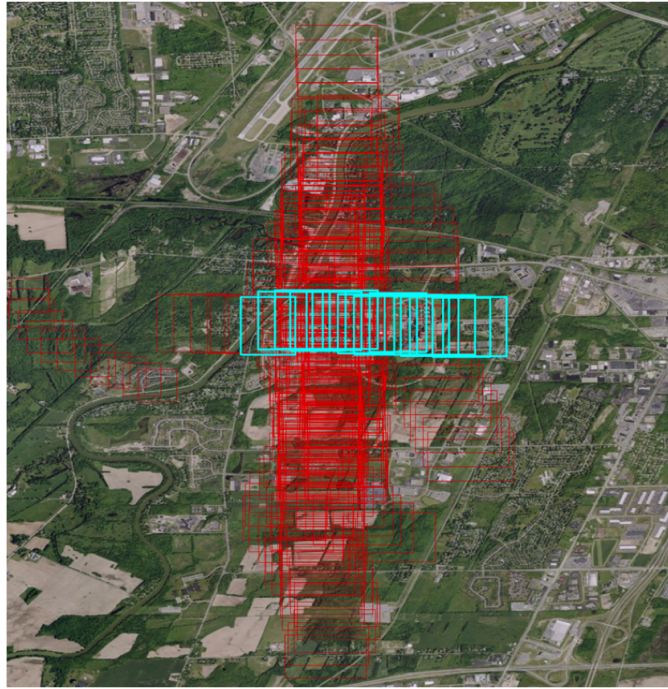


**Figure 3.24-49: Footprints of 14 images collect with the RIT WASP sensor of the RIT campus used to create a 3D point cloud.**

- The introduction of an ASCII/Text import tool to help users import simple data files into the material editor (spectral reflectance, emissivity, extinction, etc. curves) and platform editor (relative response functions, spectrometer center/widths, etc.).
- The introduction of a “simulation preview” tool that helps a user visualize a complex data collection in a real-time graphical presentation.
- The development of simple image viewer to allow users to quickly visualize generated imagery.
- The development of a large number of pre-packaged “demonstrations” to provide end-users with examples of how to use specific features and a streamlined HTML index to browse and access them.
- The restart of the DIRSIG blog (<http://dirsig.blogspot.com>) to help keep users informed and as a way to provide tips from the expert users at RIT.

The 4.4 releases also included two new scenes developed by Niek Sanders using recently developed plugins for Blender (<http://www.blender3d.org>). These scenes are modest in size (larger than MicroScenes but smaller than MegaScenes), but have a large amount of detail. The first scene was the “Warehouse” scene, which is a simple warehouse structure surrounded by a large amount of high spatial resolution clutter including stacks of shipping containers, crates, pallets, drainage pipe, steel, etc. (see Figures 3.25-51 and 3.25-52).

The second scene developed during the past year was the “Refinery” scene. Although the extents of the scene are fairly large (many kilometers), the area of interest is a modestly sized oil refinery in a coastal, desert location (see Figures 3.25-53 and 3.25-54).



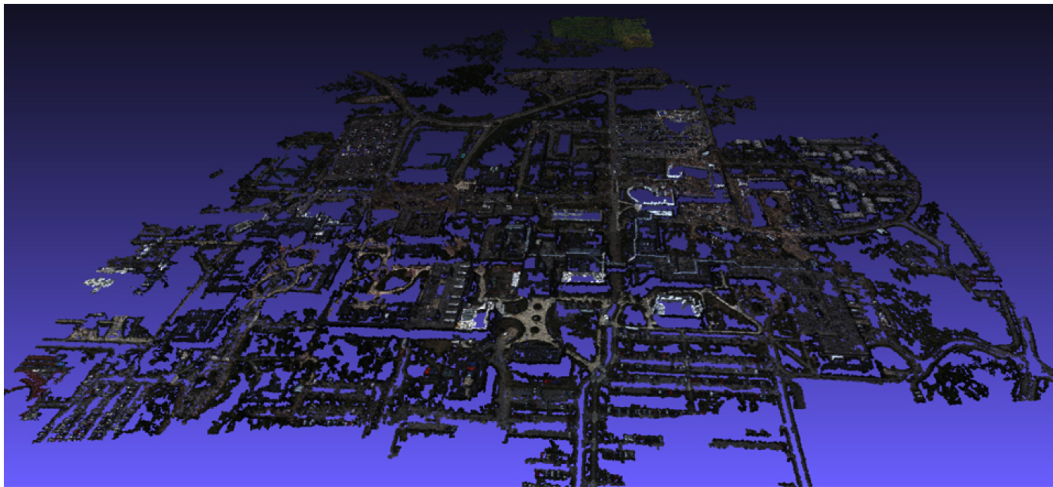


**Figure 3.24-50: An example dense point cloud displayed in MeshLab that was produced from the collect airborne images of the RIT campus.**

During the next year, the development team will continue to provide the user community with improved versions of the DIRSIG model with an increased focus on integration into the modeling workflows used by the user community. This upcoming year will also see more enhancements to the user interface, improved documentation and outreach to educate the user community and the expansion of off-site training sessions to make training more accessible.

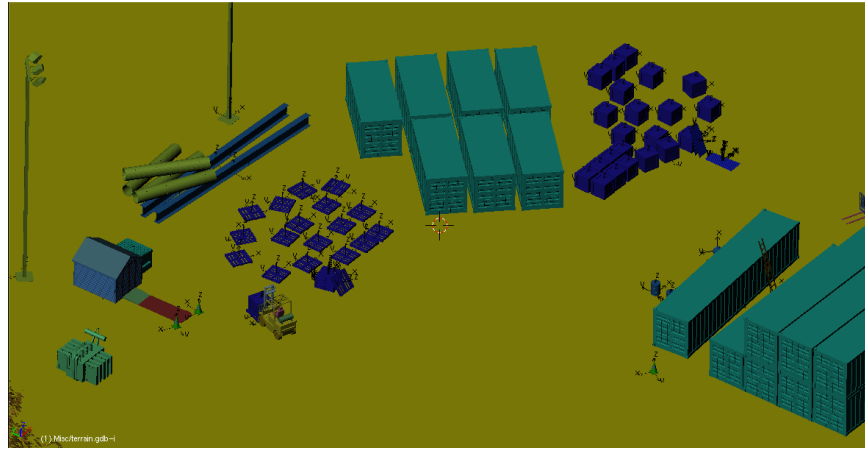


Figure 3.25-51: Screen shots of the new “warehouse” scene in Blender featuring some of the detailed clutter in the scene.

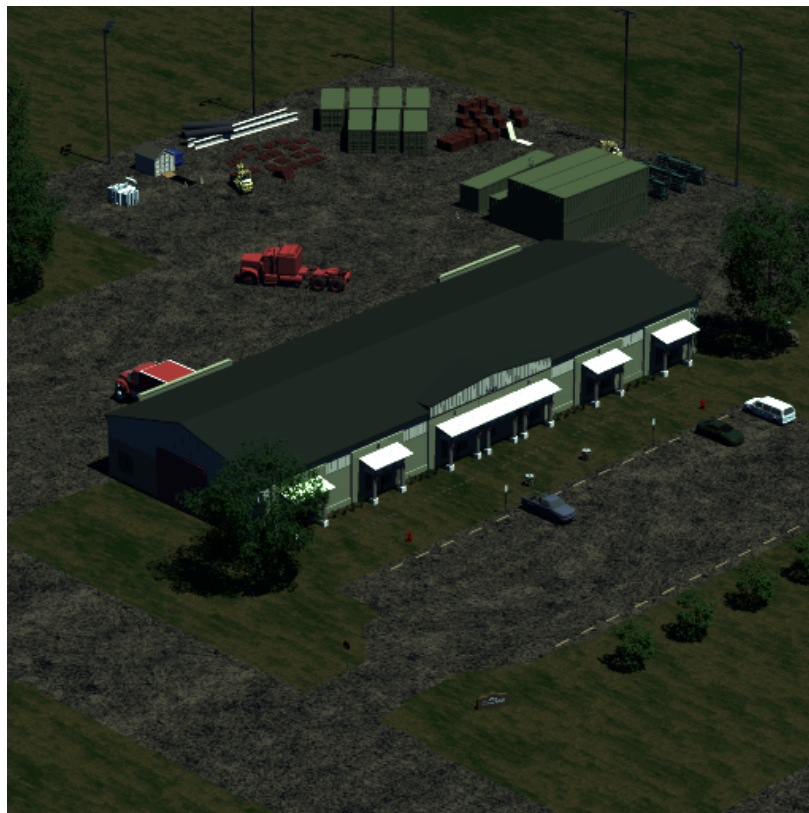


Figure 3.25-52: An RGB rendering of the “warehouse” scene by DIRSIG.

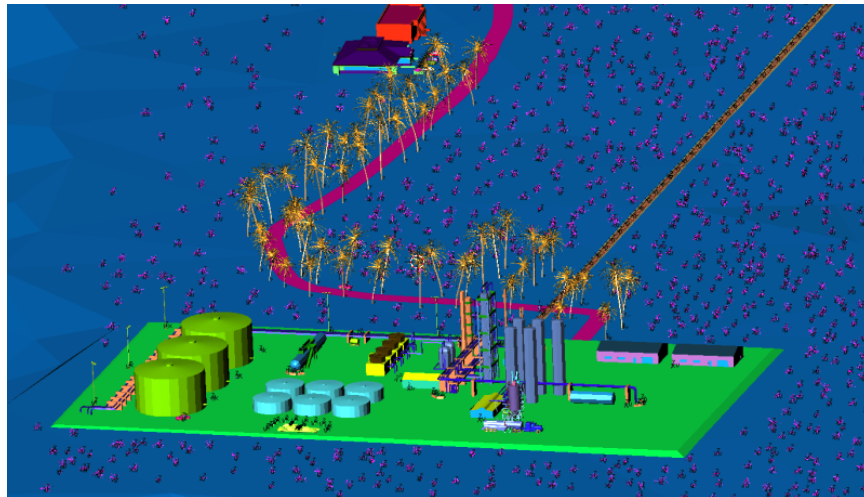
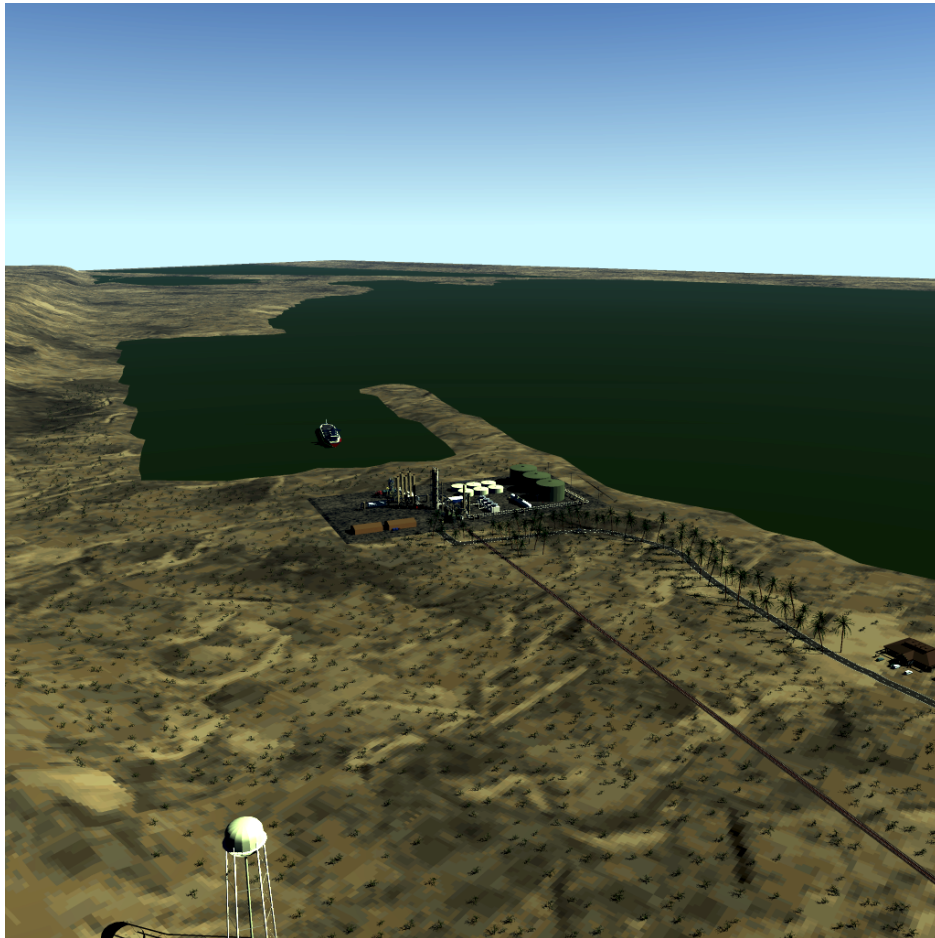


Figure 3.25-53: Screen shots of the new “refinery” scene in Blender featuring some of the detailed clutter in the scene.



**Figure 3.25-54: An RGB rendering of the “refinery” scene by DIRSIG.**

### 3.26 Advanced Radiosity Reflectance Retrieval Support

Sponsor: Air Force Research Laboratory, Ball Aerospace

Principal Investigator(s): Dr. Michael Gartley

Research Team: Dr. Adam Goodenough

Project Description:

This project was a continuation of a previous collaboration with Ball and AFRL focusing on the improvement of existing tools using the concept of Adjoint Radiosity for retrieving the surface reflectance of targets under complex illumination conditions. RIT's focus during this phase was to provide modeled hyperspectral cube datasets, experimentally collected hyperspectral cube datasets containing surfaces hidden from the view of the camera exhibiting adjacency effects on surfaces visible to the camera. Additionally, RIT also implemented its previously developed atmospheric point spread function generation code from a spreadsheet based Mathcad model to a MATLAB implementation to seamlessly work within the Ball developed exploitation workflow. Finally, RIT researched and developed novel methods for deciding on a minimalist facetization of a complex scene geometry description (either in raster or point cloud form) in order to aid in the reflectance retrieval exploitation chain.

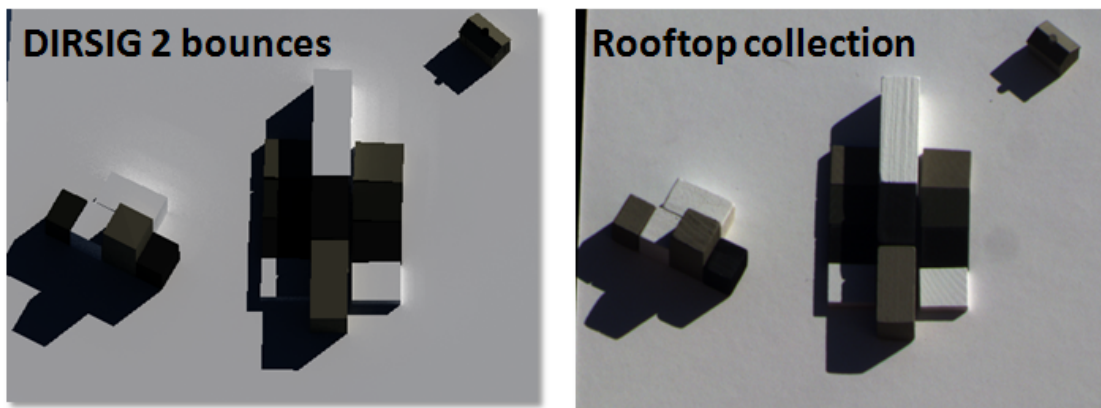


**Figure 3.26-55: Examples of a modeled and an experimental dataset provided to sponsor in support of algorithm development.**

Project Status:

This phase of the project is complete with potential for a follow-on task during the upcoming year to continue the efforts with a focus on BRDF specific phenomenology and handling of vegetation canopies within the facetization algorithm.

### 3.27 Large Area Polarimetric Scene Simulation and Phenomenology

Sponsor: Sandia National Laboratory

Principal Investigator(s): Dr. Michael Gartley

Research Team: Chris DeAngelis, Erin Ontiveros

#### Project Description:

The goal of this research effort was to improve RIT's modeling capabilities to support the generation of large spatial extent ( $\approx 100 \times 100$ km) synthetic polarimetric image datasets. The typical workflow consisted of creating a triangulated interconnected network representation of a NASA SRTM 30m digital elevation model in true geodetic coordinates. The resulting terrain is then attributed with a material classification map to discriminate vegetation, urban areas, water, and agricultural locations. Within each material class, a 15m LANDSAT-7 image was utilized to generate spatial texture.

The polarized bi-directional distribution function properties of each material class were leveraged from publically available polarimetric signatures existing in the POLDER/PARASOL BRDF databases provided by the European Space Agency. Additionally, polarized MODTRAN4 is utilized to perform polarized radiative transfer between a space based camera and the ground terrain. A voxelized, polarimetric cloud radiative transfer model was also initiated under this effort (see figure 3.27-56).

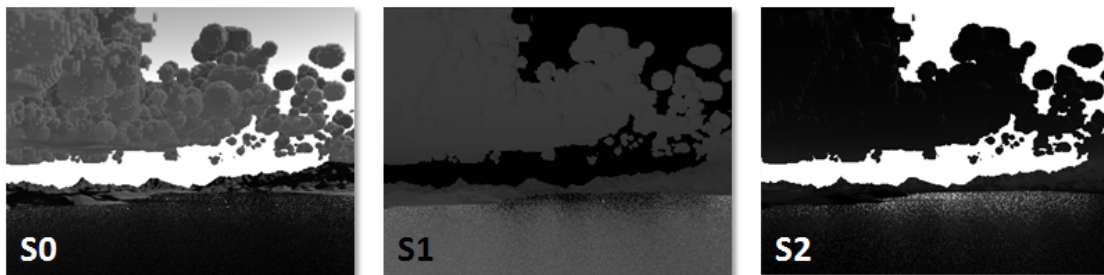


Figure 3.27-56: Example ground level view of a large scale polarimetric DIRSIG scene.

Another focus within this research was to examine the potential utility of procedural tools, such as CityEngine, to generate realistic large scale man-made clutter by providing open source street maps of the modeled region.

#### Project Status:

Although still ongoing, this project has so far been successful at defining a simplified workflow for generating large spatial extent scenes leveraging readily available SRTM elevation models, LANDSAT imagery and POLDER/PARASOL BRDF database signatures. Generation of realistic man-made ground clutter continues to be a challenging problem, with moderate success being found utilizing the procedural tool CityEngine in conjunction with Open Street Map road networks.

### 3.28 SOFIA Data Cycle System Development & Support

Sponsor: University Space Research Association (USRA), National Aeronautics and Space Administration (NASA)

Principal Investigator(s): Mr Bob Krzaczek

#### Project Description:

The Stratospheric Observatory For Infrared Astronomy (SOFIA) is the premier infrared and sub-millimeter observatory in the next two decades for astronomers around the world. Jointly developed by NASA and DLR (the German Aerospace Center), SOFIA represents the next generation of airborne observatories. A Boeing 747SP aircraft has been modified to carry a 17 ton telescope whose primary mirror is 100 inches

in diameter to altitudes as high as 45,000 feet, where it makes sensitive measurements of a wide range of astronomical objects. At these stratospheric altitudes, the telescope and its suite of scientific instruments can collect radiation in wavelengths from 0.3 to 1,000 micrometers.

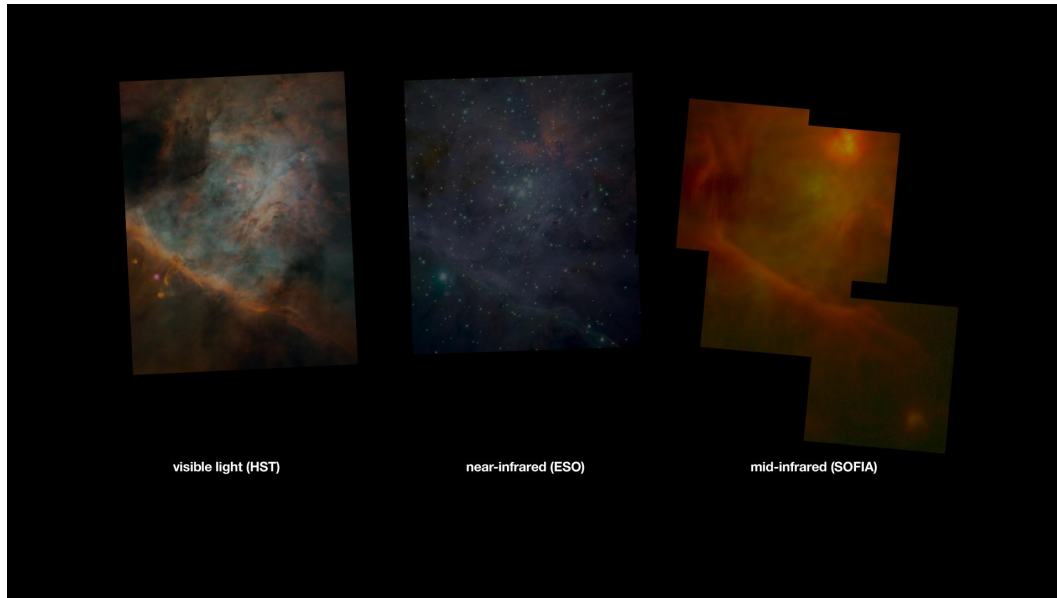


**Figure 3.28-57: SOFIA mid-infrared image of the Orion Bar in M42, complementing imagery captured by other facilities. Note the details and structure revealed in the upper portion of the image, not visible at other wavelengths. (Obtained using Cornell’s FORCAST instrument on SOFIA.)**

A key component of NASA’s program to explore fundamental questions about the universe, SOFIA will help astronomers learn more about the birth of stars, the formation of solar systems, the nature and evolution of comets, the origin of complex molecules in space, how galaxies form and change, and the nature of the mysterious black holes lying at the centers of many galaxies including our own.

The Data Cycle System (DCS), originally designed by RIT for USRA, provides the formal structure for the “observation life-cycle” required by any major astronomical observatory. From the proposal of astronomical targets, the selection of scientific instruments, the design of those observations, the scheduling of missions, the execution of those observations, the automated reduction of the raw data, to the dissemination of those data products to its users around the world, the DCS enables a global community of astronomers to interact with this new observatory entirely at a distance.

#### Project Status:

SOFIA has graduated from first light and test flights to begin delivering on its first class promises in infrared astronomy. The observatory is now making several flights every week, and has rotated through a number of instruments, acquiring data in a variety of different modalities and wavelengths. Already, SOFIA has yielded new data revealing structures in distant nebula, evidence for previously undetected molecules in space, even the fortuitous stellar occultation of a magnitude 14 star by Pluto, revealing new details about its atmosphere.

Throughout 2011’s observations, the DCS managed the transfer, archival, and dissemination of raw science data, taken from the different instruments available on SOFIA to a worldwide audience. Building on the Basic Science call for proposals in 2010, this year the DCS is successfully managing the Call for Propos-

als for Science Cycle 1, a landmark in any observatory such as SOFIA. Surprisingly, the size of the data gathered by the observatory grew much larger and faster this year than was previously anticipated by the various instrument teams; in response, key portions of the DCS were redesigned and re-implemented on an accelerated schedule, where we delivered a 30× performance boost to end-of-flight activities.

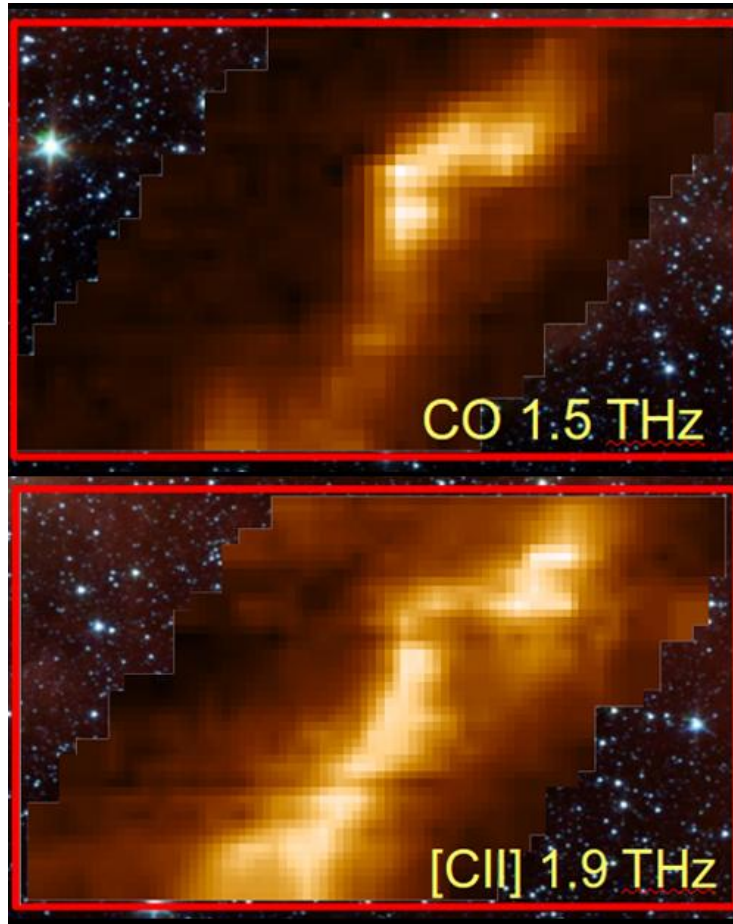


**Figure 3.28-58: Terahertz spectroscopy of the star forming region M17, superimposed on a near-infrared image, showing the spectra of ionized carbon (CII) and warm carbon monoxide (CO). (Obtained by the DLR GREAT instrument on SOFIA.)**

Presently, DCS version 2.0, focusing on the ingestion, archival, and dissemination of raw science data has been delivered to NASA, and work is beginning on version 2.1. The primary challenge of this new work will be the automation of data reduction pipelines for facility science instruments operated by the observatory. Traditionally, raw science data is processed (or “reduced”) into science products manually; the frequency of SOFIA flights and anticipated volume of data make these typical approaches unlikely to support the observatory’s aggressive schedule in 2012 and beyond. With DCS 2.1, we intend to automate much of the required post-flight calibration and data processing, freeing analysts and other personnel for other science tasks.



### 3.29 Rx-Cadre Experiments

Sponsor: USDA Forest Service, Northern Research Station

Principal Investigator(s): Dr. Robert Kremens

Project Description:

As part of the ongoing RX-CADRE experimental program (Prescribed Fire Combustion Atmospheric Dynamics Research Experiments) organized by the US Air Force, USDA Forest Service, Department of the Interior Fish and Wildlife Service, Jones Ecological Research Center, Georgia Forestry Commission, San Jose State University, University of Idaho, University of Montana and the Rochester Institute of Technology, we performed three prescribed fire experiments at Eglin AFB in the panhandle of Florida. The RIT team used the WASP aircraft sensor to collect high resolution time resolved infrared images of the progression and intensity of the fire. RIT also assisted in conducting the ignition operation on two of the three fires, the last fire being ignited from overhead by helicopter. The RIT overhead data is calibrated using in-fire overhead dual-band infrared sensors that can simultaneously measure the effective temperature of the fire, the emissivity-area product, and the radiant flux density from the fire. We developed a new suit of ground-based overhead infrared sensors for these fires that are smaller, cheaper and easier to deploy than the previous version. We were able to use up to 20 sensors on a fire, compared with 2-4 sensors on previous fires. The increased number of sensors provided more reliable calibration of the overhead sensor and also a unique data set at very high temporal resolution (5s sampling time).

Project Status:

The data from these experiments is currently being analyzed.

### 3.30 Development of 3-dimensional Air Flow Sensors for Combustion Research

Sponsor: USDA Forest Service, Northern Research Station

Principal Investigator(s): Dr. Robert Kremens

Research Team: Matthew Hart (Notre Dame), Timothy Miller (CD, RIT), Anna Higgs (EMT, RIT)

Project Description:

Measurement of the 3-dimensional wind field is critical to the understanding movement of thermal energy throughout the wildland fire environment. Flow plus fluid temperature (density) gives information about convective energy transport, the dominant mode of energy transport within wildland fires. In general, flow measurements have either been made outside the fire with 3-dimensional sensors or in the fire with 1- or 2-dimensional sensors. In all cases, these measurements have only been made at a very few (order of 5) locations within the fire. Contrast this to the measurement of radiant flux, which has been performed in-fire with 20-30 sensors and overhead using imaging technology (equivalent to 100s of thousands of sensors).

Current technologies include vane/cup anemometers (2-dimensional), sonic anemometers, and various differential pressure probes (Pitot or static tube sensors). For this project we developed and characterized a 3-dimensional wind sensor using, partially, an existing design<sup>1</sup> along with modern electronics and computer flow modeling to obtain optimum sensor placement. The sensor packages were characterized experimentally for sensitivity and angular resolution in an RIT low Reynolds number wind tunnel. We expect this project to lead to the construction of 50-100 similar sensors for future fire experiments both by RIT researchers and their collaborators.

### 3.31 Enhanced Infrared and LIDAR Capabilities for Wildland Fire Research

Sponsor: USDA Forest Service, Northern Research Station

Principal Investigator(s): Dr. Robert Kremens

Research Team: Jessica Maben (CIS - BS)

Project Description:

The goal of this work is to enhance the capabilities of the USDA FS and RIT to analyze and interpret wildland fire data obtained from airborne data collection platforms. The airborne data has been collected using a combination of time-resolved infrared imagery and pre- and post- fire LIDAR. This modality can provide unique synoptic views of the fire ground with high spatial ( $\approx$  m) and temporal ( $\approx$ 100 s) resolution. This data cannot be obtained using other methods, and to date has not been obtained except in this experiment. We have a very unique data set. We obtained this highly instrumented data set for a prescribed fire in the NJ Pine Barrens near Lakewood, NJ in the spring of 2011. We are developing software tools to perform the following tasks in a semi-automatic fashion:

1. Compare fuel consumption measurements and estimates obtained from conventional field sampling methods, LIDAR and integrated heat output.
2. Investigate the fuel consumption patterns produced. We will use standard landscape ecology metrics such as shape, connectivity, area, and diversity. We will attempt to correlate these patterns, both time-integrated and as a function of time, with the underlying landscape characteristics (fuel load, slope, wind direction, ignition patterns, moisture, soil composition, etc.)
3. Model the time history of the fire using FARSITE or another fire behavior prediction code and compare with the actual fire history obtained using time-resolved infrared imaging.

### 3.32 Precision Wildland Fuel Fire Experiments

Sponsor: USDA Forest Service, Rocky Mountain Research Station

Principal Investigator(s): Dr. Robert Kremens

Project Description:

Last year we outlined experimental campaigns to measure the remote sensing observables from wildland fire combustion. These observables include the angular, temporal and spectral distribution of radiation, and measurements related to these fundamental measures such as flame emissivity, self-absorption, and measurement of the radiative fraction. We discussed at length the importance of these measurements for remote sensing of wildfires as well as for fundamental physics measurements of a basic nature.

Experiments are well underway to measure the angular distribution of the flames from combustion of both liquid and wildland fuel materials. Our groups have independently measured wildland fire from overhead (RIT) and side-on (RMRS) views under the assumption that the radiation from wildland fire is isotropic, but this has not been proved in experiments. We will employ on the order of 15 very narrow angle radiometers located a known, fixed distance from the fire center to perform these measurements. We will also use horizontal and overhead viewing infrared cameras as alternate methods of determining the angular distribution, at least from two views (overhead and side-on). The radiometers have been prototyped and built and the mechanical support structure for the experiment has been built and tested. The experiment needs to be completed and data analyzed, but at the same time we should also plan to do experiments with

similar apparatus to measure the radiant flux (and therefore emissivity) as a function of flame thickness and maybe more importantly for remote sensing, the radiant fraction. A minimum set of apparatus for these experiments is a number of radiometers with field of view  $\leq 1$  degree (with recording digitizers), 3-axis videography and several calibrated IR framing cameras. Radiometers of several different viewing angles have been constructed and tested. We have optics for two radiometers and electronics/detectors for 15 radiometers; the remaining optics must be purchased.

The emissivity and radiant fraction experiments will use the same diagnostics as the angular distribution experiments, but will observe the fire end-on for fuel beds of different depths (for emissivity measurement) or from overhead alone (for radiant fraction). Emissivity experiments will require a long fuel bed (the  $1\text{ m} \times 3\text{ m}$  RMRS standard fuel beds would serve very well) which will be observed end-on: the variation of radiant flux with flame thickness will be a measure of the emissivity of the flames. For the radiant fraction experiments we will vary the fuel loading and observe the relationship between fuel loading and total radiation release (integral of the power over the duration of the fire). Either Medtherm or wide field-of-view dual band radiometers (or both) may be used for the radiant fraction experiments. The apparatus and diagnostics are very similar for all these experiments. Experimental set up diagrams are shown in Figure 3.32-59, Figure 3.32-59, Figure 3.32-59 for angular distribution, emissivity and radiant fraction experiments, respectively.

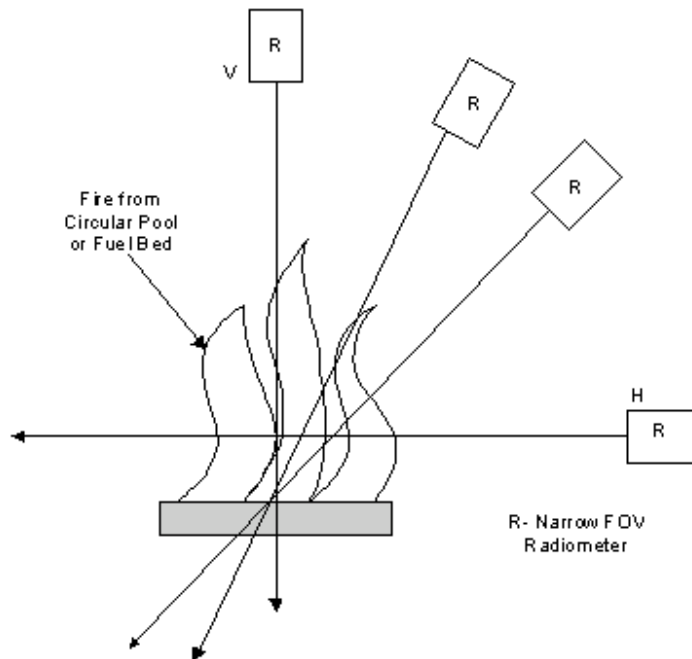


**Figure 3.32-59: Diagram of the angular distribution experiment. The narrow angle radiometers are labeled R. There are 10 radiometers, one at 0 deg., 3 at 5 deg., 3 at 45 deg., and 3 at 80 deg. Not shown are the overhead infrared camera, and three filtered (NIR) video cameras for synchronized observation of the fire plume.**

Project Status:

The angular distribution experiments were completed in June 2011, the other experiments being planned for early 2012 at the USFS Missoula Fire Science Laboratory in Missoula, MT.

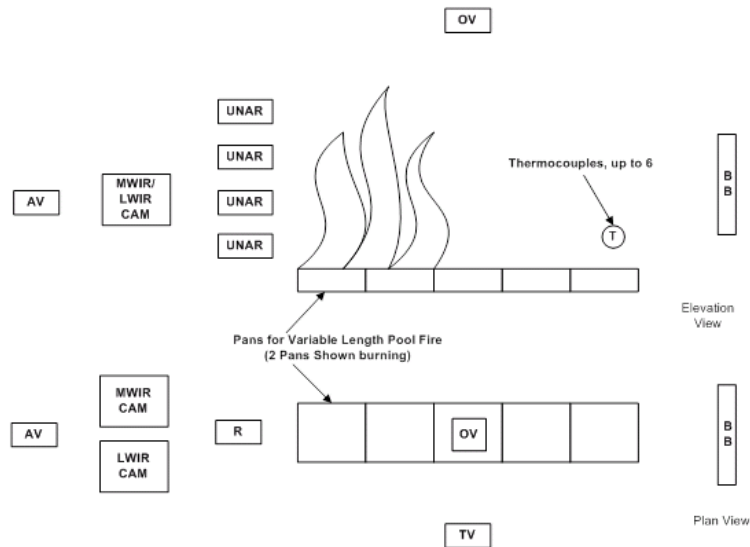


Figure 3.32-60: Diagram of the emissivity experiment. UNAR ultra narrow angle radiometer ( $\approx 0.50$ ); OV-overhead view video camera; TV transverse view video camera; AV axial view video camera; BB-blackbody reference for IR cameras.

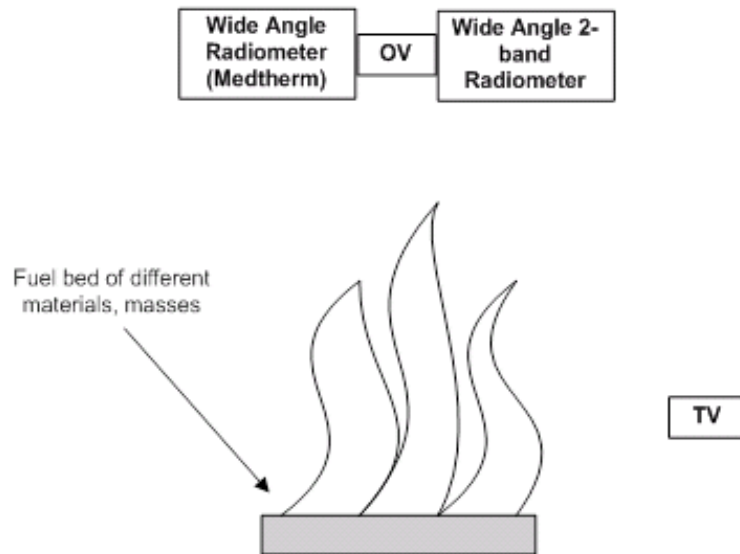


Figure 3.32-61: Diagram of the radiant fraction experiment. OV- overhead view video camera; TV transverse view video camera. The mass of the fuel bed is varied to observe the partition between radiation and total fuel mass over a wide range of fuel masses.

### 3.33 Improved Diagnostics for Fire-Initiation Experiments

Sponsor: USDA Forest Service, Northern Research Station

Principal Investigator(s): Dr. Robert Kremens

Project Description:

The ability to predict and model fire initiation is critical to improving the reliability and accuracy of fire-behavior modeling codes. A long-held notion is that radiation from the fire front ignites the fuel bed so that radiation is the dominant energy transfer mechanism for fire initiation. Recent laboratory experiments at RMRS have shown that convective cooling can carry away enough energy from the fuel bed that radiative heating is ineffective. Other experiments have shown that convection is the dominant mode of fire spread in wildland fuel materials, and in fact, direct working fluid (flame) contact is necessary for reliable ignition of fuels in front of the flaming combustion zone, especially for low-to-moderate intensity fires. RMRS has several research instrumentation needs to further these investigations. The ability to visualize the convective flow and to determine the presence of laminar vs. turbulent flow would add credibility to the argument that convective cooling wins over radiative heating. Schlieren shadowgraph photography has long been used as a diagnostic for detection of density variations in and around objects. This method produces a qualitative observation that could show the onset of turbulence and the transition from laminar to turbulent flow around wildland fuel particles. If shadowgraphy is correlated in time with other measurements radiative flux, temperature measurements at the fuel particle surface, etc. significant advances may be made with regard to the initiation question. Our intent is to develop a versatile system of both radiometric and qualitative diagnostics to study the onset of combustion in wildland fuel materials. The goal of the experiment is to both to provide a known uniform flux to an experimental volume and also to measure both radiative and convective energy flow in the experimental volume. I believe it is necessary to move to a carefully controlled beam geometry to study these subtle effects. Using a well characterized source can remove the effects of source non-uniformities from other real effects. This project will consist of but not be limited to the following:

1. Schlieren photographic system consisting of a high resolution ( $\leq 1$  mm) shadowgraph system and 30Hz recording with a high quality video system<sup>2</sup>
2. Radiant power delivery system consisting of focusing optics and radiant source (possible from RMRS panel heaters or electric heat sources (globar)) to deliver power in excess of 60 kW/m<sup>2</sup> to a volume 100 cm<sup>3</sup>. The power will be easily variable from 5- $\leq$  60 kW/m<sup>2</sup>. The power in the focal volume will be uniform.
3. Radiant power measurement system synchronized with Schlieren observations using narrow angle radiometers or calorimeters.
4. Conventional videography in deep NIR (800nm) synchronized with Schlieren observations. Observation at these long wavelengths eliminates background illumination and allows for better timing of the onset of combustion of the wildland fuel materials.

A diagram of the experimental set up is given in Figure 3.33-62.

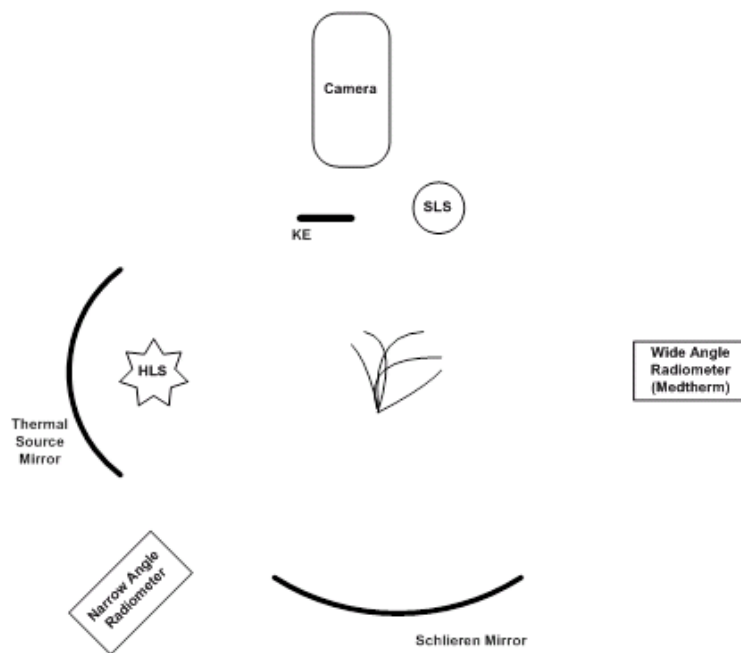


Figure 3.33-62: Experimental layout of the initiation experiment. SLS-Schlieren point light source; HLS-High intensity light source; KE- knife edge. The field of view of the narrow angle radiometer is adjusted to be equal to the angle subtended by the sample volume. The thermal source mirror concentrates and collimates the radiation from the high intensity light source. IR videography of the sample volume is not shown.

## 4 Publications During This Period

- [1] A. O. Rivas, "Tunable micro-electro mechanical fabry perot etalon," m.s. thesis, Rochester Institute of Technology, College of Science, Center for Imaging Science, Rochester, New York, United States, August 2011.
- [2] C. R. Anderson, *Refinement of the Method for Using Pseudo-Invariant Sites for Long Term Calibration Trending of Landsat Reflective Bands*. Ph.d. dissertation, Rochester Institute of Technology, College of Science, Center for Imaging Science, Rochester, New York, United States, 2011.
- [3] X. Fan, *Automatic Registration of Multi-Modal Airborne Imagery*. Ph.d. dissertation, Rochester Institute of Technology, College of Science, Center for Imaging Science, Rochester, New York, United States, 2011.
- [4] B. M. Flusche, *An Analysis of Multimodal Sensor Fusion for Target Detection in an Urban Environment*. Ph.d. dissertation, Rochester Institute of Technology, College of Science, Center for Imaging Science, Rochester, New York, United States, 2011.
- [5] M. D. Presnar, *Modeling and Simulation of Adaptive and Multimodal Optical Sensors for Target Tracking in the Visible to Near Infrared*. Ph.d. dissertation, Rochester Institute of Technology, College of Environmental Science & Forestry, Center for Imaging Science, Rochester, New York, United States, 2011.
- [6] J. A. Speir, *Validation of 3D Radiative Transfer in Coastal Ocean-Water Systems as Modeled by DIRSIG*. Ph.d. dissertation, Rochester Institute of Technology, College of Science, Center for Imaging Science, Rochester, New York, United States, 2011.
- [7] A. J. Spivey, *Land Cover Land Use Change Index Interpretation for the Persistent Monitoring of Riparian System Landscape Pattern When Using Multiple Sensor Scales*. Ph.d. dissertation, Rochester Institute of Technology, College of Science, Center for Imaging Science, Rochester, New York, United States, 2011.
- [8] A. M. Weiner, *A Systems Level Characterization and Tradespace Evaluation of a Simulated Airborne Fourier Transform Infrared Spectrometer for Gas Detection*. Ph.d. dissertation, Rochester Institute of Technology, College of Science, Center for Imaging Science, Rochester, New York, United States, 2011.
- [9] C. Devaraj, *Polarimetric Remote Sensing System Analysis: DIRSIG Model Validation and Impact of Polarization Phenomenology on Material Discriminability*. Ph.d. dissertation, Rochester Institute of Technology, College of Science, Center for Imaging Science, Rochester, New York, United States, September 2010.
- [10] K. C. Walli, *Relating Multimodal Imagery Data in 3D*. Ph.d. dissertation, Rochester Institute of Technology, College of Science, Center for Imaging Science, Rochester, New York, United States, August 2010.
- [11] J. Wu, J. A. van Aardt, and G. P. Asner, "A comparison of signal deconvolution algorithms based on small-footprint lidar waveform simulation," *IEEE Transactions on Geoscience and Remote Sensing* **49**, pp. 2402–2414, June 2011.
- [12] W. J. Roberts, J. A. van Aardt, and F. Ahmed, "Image fusion for enhanced forest structural assessment," *International Journal of Remote Sensing* **32**, pp. 243–266, January 2011.
- [13] K. Wessels, R. Mathieu, B. F. Erasmus, G. P. Asner, I. P. Smit, J. A. van Aardt, R. Main, J. Fisher, W. Marais, T. Kennedy-Bowdoin, D. Knapp, E. R., and J. J., "Impact of communal land use and conservation on woody vegetation structure in the lowveld savannas of south africa," *Forest Ecology and Management* **261**, pp. 19–29, January 2011.
- [14] E. J. Ientilucci and P. Bajorski, "Hyperspectral target detection in a whitened space utilizing forward modeling concepts," *Workshop on Hyperspectral Image and Signal Processing: Evolution in Remote Sensing* **1**, June 2010.

- [15] P. Bajorski, "Second moment linear dimensionality as an alternative to virtual dimensionality," *IEEE Transactions on Geoscience and Remote Sensing* **2**(49), pp. 672–678, 2011.
- [16] P. Bajorski, "Statistical inference in PCA for hyperspectral images, *IEEE Journal of Selected Topics in Signal Processing*," *IEEE Signal Processing* **3**(5), pp. 438–445, 2011.
- [17] P. Bajorski, "Generalized detection fusion for hyperspectral images" *IEEE Transactions on Geoscience and Remote Sensing* (Issue: 99), pp. 1–7, 2011.
- [18] D. R. Nilosek and C. Salvaggio, "Applying computer vision techniques to perform semi-automated analytical photogrammetry," *IEEE Xplore* , pp. 1–5, November 2010.
- [19] B. D. Bartlett, M. G. Gartley, D. W. Messinger, C. Salvaggio, and J. R. Schott, "Spectro-polarimetric bidirectional reflectance distribution function determination of in-scene materials and its use in target detection applications," *Journal of Applied Remote Sensing* **4**, pp. 1–21, November 2010.
- [20] F. P. Padula and J. R. Schott, "Historic calibration of the thermal infrared band of landsat-5 tm," *Photogrammetric Engineering and Remote Sensing* **76**, pp. 1225–1238, November 2010.
- [21] B. Flusche, M. G. Gartley, and J. R. Schott, "Assessing the impact of spectral and polarimetric data fusion via simulation to support multimodal sensor system design requirements," *Journal of Applied Remote Sensing* **4**, November 2010.
- [22] M. A. Cho, P. Debba, R. Mathieu, L. Naidoo, J. A. van Aardt, and G. P. Asner, "Improving discrimination of savanna tree species through a multiple endmember spectral angle mapper approach: Canopy-level analysis," *IEEE Transactions on Geoscience and Remote Sensing* **48**, pp. 4133–4142, October 2010.
- [23] B. Somers, S. Delalieux, W. Verstraeten, J. A. van Aardt, G. Albrigo, and P. Coppin, "An automated waveband selection technique for optimized hyperspectral mixture analysis," *International Journal of Remote Sensing* **31**, pp. 5549–5568, October 2010.
- [24] L. Meng and J. P. Kerekes, "Adaptive target detection with a polarization-sensitive optical system, submitted for review," *Applied Optics* , October 2010.
- [25] K. Canham, A. Schlamm, A. Ziemann, B. Basener, and D. W. Messinger, "Spatially adaptive hyperspectral endmember selection and spectral unmixing," *IEEE Transactions on Geoscience and Remote Sensing* **submitted to**, October 2010.
- [26] B. M. Flusche, M. G. Gartley, and J. R. Schott, "Defining a process to fuse polarimetric and spectral data for target detection and explore the trade space via simulation," *Journal of Applied Remote Sensing* **4**, October 2010.
- [27] S. Matteoli, E. J. Ientilucci, and J. P. Kerekes, "Operational and performance considerations of radiative transfer modeling in hyperspectral target detection?, accepted for publication," *IEEE Transactions on Geoscience and Remote Sensing* , pp. 1–13, September 2010.
- [28] M. A. Cho, J. A. van Aardt, R. Main, and B. Majeke, "Evaluating variations of physiology-based hyperspectral features along a soil water gradient in a eucalyptus grandis plantation," *International Journal of Remote Sensing* **31**(12), pp. 3143–3159, 2010.
- [29] S. G. Tesfamichael, J. A. van Aardt, and F. Ahmed, "Estimating plot-level tree height and volume of eucalyptus grandis plantations using small-footprint, discrete return lidar data," *Progress in Physical Geography* **34**(4), pp. 515–540, 2010.
- [30] M. T. Gebreslasie, F. Ahmed, and J. A. van Aardt, "Predicting forest structural attributes using ancillary data and aster satellite data," *International Journal of Applied Earth Observation and Geoinformation* **12S**(2010), pp. S23–S26, 2010.



- [31] A. Schlamm, D. W. Messinger, A. Ziemann, and B. Basener, "Change detection in multi- and hyperspectral image tiles based on quantitative measures of point density," *Journal of Applied Remote Sensing*, **accepted for publication**, 2011.
- [32] F. P. Padula, J. R. Schott, J. A. Barsi, N. G. Raqueno, and S. J. Hook, "Calibration of landsat 5 thermal infrared channel: updated calibration history and assessment of the errors associated with the methodology," *Canadian Journal of Remote Sensing*, **accepted for publication**, 2010.
- [33] S. E. Paul and C. Salvaggio, "A polynomial regression approach to subpixel temperature extraction from a single-band thermal infrared image," in *Proceeding of SPIE, SPIE Defense and Security, Thermosense XXXIII, Thermal Infrared Applications*, **8013**, SPIE, (Orlando, Florida, United States), April 2011.
- [34] B. D. Bartlett, A. Schlamm, C. Salvaggio, and D. W. Messinger, "Anomaly detection of man-made objects using spectro-polarimetric imagery," in *Proceeding of SPIE, Defense and Security Symposium, Algorithms and Technologies for Multispectral, Hyperspectral, and Ultraspectral Imagery XVII, Spectral Data Analysis Methodologies I*, **8048**, SPIE, (Orlando, Florida, United States), 2011.
- [35] D. W. Messinger, J. A. van Aardt, D. McKeown, M. V. Casterline, J. W. Faulring, N. G. Raqueno, B. Basener, and M. Velez-Reyes, "High resolution and lidar imaging support to the haiti earthquake relief effort," in *Imaging Spectrometry XV, Optics & Photonics, Imaging Spectrometry XV*, **7812**, SPIE, (San Diego, California, United States), August 2010.
- [36] A. Weiner and D. W. Messinger, "An end-to-end airborne fts simulation for evaluating the performance trade space in fugitive gas identification," in *Imaging Spectrometry XV, Optics & Photonics, Imaging Spectrometry XV*, **7812**, SPIE, (San Diego, California, United States), August 2010.
- [37] B. M. Flusche, J. R. Schott, and M. G. Gartley, "Exploiting spectral and polarimetric data fusion to enhance target detection performance," in *Proceedings of the SPIE, Imaging Spectrometry XV*, **7812**, SPIE, (San Diego, California, United States), August 2010.
- [38] J. McGlinchy, J. A. van Aardt, H. E. Rhody, J. P. Kerekes, E. J. Lentilucci, G. P. Asner, D. Knapp, R. Mathieu, T. Kennedy-Bowdoin, B. F. Erasmus, K. Wessels, I. P. Smit, J. Wu, and D. Sarrazin, "Extracting structural land cover components using small-footprint waveform lidar data," in *Proceedings of 2010 IEEE International Geoscience & Remote Sensing Symposium, IGARSS, IEEE*, (Honolulu, Hawaii, USA), July 2010.
- [39] D. Simmons, J. P. Kerekes, D. Rahn, A. K. Shaw, and J. I. Medford, "Hyperspectral imaging phenomenology of genetically engineered plant sentinels," in *Proceedings of the 2010 IEEE International Geoscience and Remote Sensing Symposium, IGARSS 2010*, pp. 3386–3389, IEEE, (Honolulu, Hawaii, United States), July 2010.
- [40] M. D. Presnar and J. P. Kerekes, "Modeling and measurement of optical polarimetric image phenomenology in a complex urban environment," in *Proceedings of 2010 IEEE International Geoscience & Remote Sensing Symposium, IGARSS 2010*, pp. 4389–4392, IEEE, (Honolulu, Hawaii, United States), July 2010.
- [41] J. A. Barsi, B. L. Markham, J. R. Schott, S. J. Hook, and N. G. Raqueno, "Twenty-five years of landsat thermal band calibration," in *2010 IEEE International Geoscience and Remote Sensing Symposium (IGARSS)*, pp. 2287–2290, IEEE, (Honolulu, Hawaii, United States), July 2010.
- [42] J. P. Kerekes, "Application-driven spectral image quality assessment and prediction," in *OSA Technical Digest, Digital Image Processing and Analysis*, Optical Society of America, (Tucson, Arizona, United States), June 2010.
- [43] J. Speir, J. R. Schott, A. A. Goodenough, and S. D. Brown, "Validation of in-water 3d radiative transfer using dirsig," in *WHISPERS 2010*, IEEE, (Reykjavik, Iceland), June 2010.

- [44] J. R. Schott and A. D. Gerace, "The impact of land processes on fresh and coastal waters," Tech. Rep. 10-51-182, RIT/DIRS, Rochester, New York, United States, September 2010.
- [45] E. J. Ientilucci and J. R. Schott, *Radiometry and Radiation Propagation*, vol. In progress., Oxford University Press, Rochester, New York, United States, 1st ed., 2011.
- [46] P. Bajorski, *Statistics for Imaging, Optics, and Photonics*, Wiley, Rochester, New York, United States, 2011.
- [47] J. A. van Aardt, R. Mathieu, M. Cho, K. Wessels, B. F. Erasmus, G. P. Asner, and I. P. Smit, *Observations on Environmental Change in South Africa*, vol. 3, ch. Assessing degradation across a land use gradient in the Kruger National Park area using advanced remote sensing modalities; see: pp. 97-103. SUN PRESS, Stellenbosch, Western Cape, South Africa, 1st ed., April 2011.
- [48] J. A. van Aardt, M. Cho, R. Main, R. Mathieu, B. Somers, M. Norris-Rogers, S. Verreynne, W. Verstraeten, and P. Coppin, *Observations on Environmental Change in South Africa*, vol. 3, ch. Ecosystems: Case studies in capital intensive crops towards system modeling of ecosystems using integrated hyperspectral remote sensing and in situ inputs; see: pp. 116-123. SUN PRESS, Stellenbosch, Western Cape, South Africa, 1st ed., April 2011.
- [49] J. A. van Aardt, I. Kotze, M. Cho, R. Mathieu, and M. Norris-Rogers, *Observations on Environmental Change in South Africa*, vol. 3, ch. Species-level classification using imaging spectroscopy for the detection of invasive alien species; see: pp. 147-153. SUN PRESS, Stellenbosch, Western Cape, South Africa, 1st ed., 2011.
- [50] J. A. van Aardt, M. Vogel, W. Luck, and J. D. Althausen, *Manual of Geospatial Science and Technology*, ch. Remote sensing systems for operational and research use. In: *Manual of Geospatial Science and Technology*, Bossler J.D. (Ed.), CRC Press, Taylor & Francis, New York, 808p. CRC Press, Boca Raton, Florida, USA, 2nd ed., 2010.
- [51] M. J. Cook, F. P. Padula, J. R. Schott, and C. Cao, "Spatial, spectral, and radiometric characterization of libyan and sonoran desert calibration sites in support of goes-r vicarious calibration," Master's thesis, Rochester Institute of Technology, College of Science, Center for Imaging Science, Rochester, New York, United States, August 2010.
- [52] K. N. Salvaggio, "Phenomenological study of passive image-based observables used to determine standard from overlaid vehicles," Master's thesis, Rochester Institute of Technology, College of Science, Center for Imaging Science, Rochester, New York, United States, May 2010.
- [53] C. Salvaggio, R. V. Raqueno, A. R. Scott, and P. Y. Youkhana, "Accurate radiometric temperature measurements using thermal infrared imagery of small targets, physics-based modeling, and companion high-resolution optical image data sets," in *University and Industry Technical Interchange Review Meeting, UITI 2010, Plenary Session*, Department of Energy NA-22, (Knoxville, Tennessee, United States), December 2010.
- [54] M. J. Cook, F. P. Padula, J. R. Schott, and C. Cao, "Spatial, spectral, and radiometric characterization of libyan and sonoran desert calibration sites in support of goes-r vicarious calibration," in *Senior Research Project*, Rochester Institute of Technology, (Rochester, New York, United States), August 2010.
- [55] H. E. Rhody and R. Krzaczek, "Rit airborne imagery and lidar collection over haiti earthquake region," in *Haiti RAPIDS and Research Needs Workshop, Principal Investigator Workshop, September 30-October 1, 2010*, National Science Foundation, (Washington, DC, USA), 2010.
- [56] K. C. King and J. P. Kerekes, "Development of a web-based blind test to score and rank hyperspectral classification algorithms," in *Proceedings of the 2010 Western New York Image Processing Workshop,, IEEE*, (Rochester, New York, United States), November 2010.

- [57] A. Schlamm and D. W. Messinger, "A euclidean distance transformation for improved anomaly detection in spectral imagery," in *Proceedings of the 2010 Western New York Image Processing Workshop*, IEEE, (Rochester, New York, United States), November 2010.
- [58] R. Mercovich, A. Harkin, and D. W. Messinger, "Utilizing the graph modularity to blind cluster multispectral satellite imagery," in *Proceedings of the 2010 Western New York Image Processing Workshop*, (Rochester, New York, United States), November 2010.
- [59] Z. Lu, A. C. Rice, J. R. Vasquez, and J. P. Kerekes, "Target discrimination via optimal wavelength band selection with synthetic hyperspectral imagery," in *Proceedings of the Second Workshop on Hyperspectral Image and Signal Processing: Evolution in Remote Sensing*, IEEE, (Reykjavik, Iceland), June 2010.
- [60] M. D. Presnar, J. P. Kerekes, and D. R. Pogorzala, "Dynamic image simulations for adaptive sensor performance predictions," in *Proceedings of the Second Workshop on Hyperspectral Image and Signal Processing: Evolution in Remote Sensing*, IEEE, (Reykjavik, Iceland), June 2010.
- [61] P. Bajorski and N. J. Sanders, "A modified pixel purity index method for hyperspectral images," in *Workshop on Hyperspectral Image and Signal Processing, Evolution in Remote Sensing*, Remote Sensing and Photogrammetry Society, (Reykjavik, Iceland), June 2010.
- [62] P. Bajorski, "Investigation of virtual dimensionality and broken stick rule for hyperspectral images," in *Workshop on Hyperspectral Image and Signal Processing, Evolution in Remote Sensing*, Remote Sensing and Photogrammetry Society, (Reykjavik, Iceland), June 2010.
- [63] D. W. Messinger, A. Ziemann, B. Basener, and A. Schlamm, "Spectral image complexity estimated through local convex hull volume," in *WHISPERS 2010, WHISPERS*, IEEE, (Reykjavik, Iceland), 2010.
- [64] A. Schlamm, D. W. Messinger, and B. Basener, "Interest segmentation of hyperspectral imagery," in *WHISPERS 2010, WHISPERS*, IEEE, (Reykjavic, Iceland), 2010.